

**One-loop evolution of twist-2 generalized parton distributions**Valerio Bertone<sup>1\*</sup>, Rafael F. del Castillo<sup>2†</sup>, Miguel G. Echevarria<sup>3,4‡</sup>, Óscar del Río<sup>2§</sup>,  
Simone Rodini<sup>5,6¶</sup><sup>1</sup>*IRFU, CEA, Université Paris-Saclay, F-91191 Gif-sur-Yvette, France*<sup>2</sup>*Departamento de Física Teórica & IPARCOS, Universidad Complutense de Madrid, E-28040 Madrid, Spain*<sup>3</sup>*Department of Physics, University of the Basque Country UPV/EHU, 48080 Bilbao, Spain*<sup>4</sup>*EHU Quantum Center, University of the Basque Country UPV/EHU*<sup>5</sup>*Deutsches Elektronen-Synchrotron DESY, Notkestr. 85, 22607 Hamburg, Germany*<sup>6</sup>*CPHT, CNRS, Ecole polytechnique, Institut Polytechnique de Paris, 91120 Palaiseau, France***Abstract**

We revisit the evolution of generalised parton distributions (GPDs) at the leading order in the strong coupling constant  $\alpha_s$  for all of the twist-2 quark and gluon operators. We rederive the relevant one-loop evolution kernels, expressing them in a form suitable for implementation, and check analytically that some basic properties, such as DGLAP/ERBL limits and polynomiality conservation, are fulfilled. We also present a number of numerical results obtained with a public implementation of the evolution in the library **APFEL++** and available within the **PARTONS** framework.

---

<sup>\*</sup>valerio.bertone@cea.fr<sup>†</sup>raffer06@ucm.es<sup>‡</sup>miguel.garciae@ehu.eus<sup>§</sup>oscar03@ucm.es<sup>¶</sup>simone.rodini@desy.de

# Contents

<b>1</b>	<b>Introduction</b>	<b>2</b>
<b>2</b>	<b>Definitions</b>	<b>3</b>
<b>3</b>	<b>Analytic results</b>	<b>6</b>
3.1	DGLAP limit . . . . .	10
3.2	ERBL limit . . . . .	10
3.3	Continuity at $x = \xi$ and spurious divergences . . . . .	12
3.4	Sum rules . . . . .	13
3.5	Conservation of polynomiality . . . . .	14
<b>4</b>	<b>Numerical results</b>	<b>15</b>
<b>5</b>	<b>Conclusions</b>	<b>18</b>
<b>A</b>	<b>GPD evolution kernel integrals</b>	<b>19</b>
A.1	Quark-in-quark GPD . . . . .	19
A.2	Gluon-in-gluon GPD . . . . .	21
A.3	Quark-in-gluon and gluon-in-quark GPDs . . . . .	22

## 1 Introduction

Generalised parton distributions (GPDs) were introduced more than two decades ago as a natural generalisation of parton distribution functions (PDFs) [1–6] (see also Refs. [7–12] for comprehensive reviews). While PDFs are typically accessed through inclusive processes, such as deep-inelastic lepton-hadron scattering, GPDs emerge from the factorisation of deeply-virtual exclusive processes, with deeply-virtual Compton scattering (DVCS) being the golden channel [2, 3, 5]. In the DVCS amplitudes, GPDs are encoded in Compton Form Factors (CFFs) through their convolution over the longitudinal partonic momentum fraction  $x$  with known perturbative kernels [13–17].

GPDs provide a 1+2 dimensional picture of the partonic structure of hadrons related to both the longitudinal-momentum and the transverse-spatial distribution of partons [18]. Furthermore, the second Mellin moments of unpolarised GPDs give access to the so-called Ji spin sum rule [2] and the  $D$ -term, which encode information on the mechanical properties of hadrons [19–23]. In general, GPDs contain a wealth of information on hadron structure that has led the upcoming Electron-Ion Collider (EIC) [24] and the JLab22 upgrade [25] to make the study of GPDs a cornerstone of their research programs.

However, the phenomenological study of GPDs presents us with many challenges. One of the primary hurdles in extracting meaningful information from experimental data lies in the intricate structure of the factorisation theorems, which renders the analysis of GPDs considerably more difficult than that of PDFs. A pivotal aspect in the exploration of GPDs concerns the ability to disentangle their dependence on both the partonic longitudinal-momentum fraction  $x$  and the skewness  $\xi$ . This task proved exceptionally challenging in that the convolution of GPDs with the partonic cross sections involved in the computation of CFFs intertwines these variables, preventing a straightforward separation. The longstanding belief that evolution effects may help achieve this separation was finally disproven in Ref. [26], where the concept of “shadow” GPDs, *i.e.* GPDs having an arbitrary small imprint on CFFs, was introduced. However, more recently Ref. [27] revived this debate. Nonetheless, it is broadly accepted that a solid extraction of GPDs should not only rely on DVCS data but rather on a simultaneous analysis of different processes, as routinely done for PDFs.

This underscores the rationale behind the substantial efforts invested in recent years to derive the perturbative structure of both the CFFs and the evolution kernels governing the evolution of GPDs [13–17, 28, 29, 29–38]. This pursuit has driven extensive investigations into

the computation of higher-order results, primarily employing conformal-space techniques. This approach, not only enhances computational efficiency, but also offers an independent alternative to the more traditional Feynman-diagram-based methods.

On the phenomenological side, comparatively much less effort has been devoted to developing GPD evolution codes. The first leading-order (LO) momentum-space evolution code was developed by Vinnikov and presented in Ref. [39]. However, the only surviving public version of this code is available only through PARTONS [40]. Freund and McDermott [41] implemented a version of GPD evolution specifically tailored for DVCS at next-to-LO (NLO) accuracy. However, the code is not fully open-source and cannot be easily obtained. On the other hand, a public, open-source implementation of GPD evolution in conformal space at NLO also exists [28, 42, 43].

All codes mentioned above are typically able to evolve only specific models or class of parameterisations, and can thus hardly be used out-of-the-box with arbitrary input GPDs. This is a significant shortcoming in view of a possible extraction of GPDs from experimental data based on flexible parameterisations. Another disadvantage of these codes is that none of them includes heavy-flavour threshold crossing. This is a limitation because much of the current experimental data lies significantly above the charm threshold and, all the more so, the future EIC will deliver data that will require charm and bottom to be treated as active flavours. It is therefore clear that the lack of open-source public codes to perform GPD evolution in momentum space without any assumption on the initial-scale model is now becoming a bottleneck.

With this work, we aim to provide a fully open-source implementation for all of the twist-2 GPD evolution equations in momentum space with no a-priori assumptions on the input models and allowing for heavy-flavour threshold crossing. We extend the work of Ref. [44], devoted to the one-loop evolution of unpolarised GPDs, re-computing and implementing the evolution kernels for longitudinally polarised quarks and gluons, and for transversely polarised quarks and circularly polarised gluons. These quantities had already been computed (see *e.g.* Refs. [7, 45]), but a numerical implementation only exists for longitudinally polarised partons [39] (with the limitations discussed above) and was absent so far for transversely polarised quarks and circularly polarised gluons. The implementation of the full set of twist-2 evolution equations is made public through the code APFEL++ [46, 47] and available within the numerical framework PARTONS [40].

The paper is organised as follows. In Sect. 2, we give a brief overview of definitions and conventions on both the structure of GPDs and their evolution equations. The explicit form of the leading-order kernels is given in Sect. 3 and presented in a form that is well-suited for numerical implementation. In the same section, we also discuss some relevant properties of the kernels. In Sect. 4, we present some numerical results of our implementation, and finally in Sect. 5 we draw some conclusions.

## 2 Definitions

Let us first start with a summary of our notation. We will denote scalar products as  $a^\mu b_\mu \equiv (ab)$ . We introduce two light-cone vectors,  $n$  and  $\bar{n}$ , such that  $n^2 = \bar{n}^2 = 0$  and  $(\bar{n}n) = 1$ . We parametrise the transverse space to  $n$  and  $\bar{n}$  in terms of two vectors  $R$  and  $L$  that satisfy the normalisation conditions:<sup>\*</sup>

$$(RR) = (LL) = (Rn) = (Ln) = (R\bar{n}) = (L\bar{n}) = 0, \quad (RL) = -1. \quad (2)$$

In addition, we will use the short-hand notation:  $v_+ = (vn)$ ,  $v_- = (v\bar{n})$ ,  $v_R = (vR)$  and  $v_L = (vL)$  throughout.

The bare quark and gluon GPD correlators associated with the hadron  $H$  are defined in terms of off-forward matrix elements of the collinear operators as follows (see *e.g.* Ref. [8] for

---

<sup>\*</sup>An explicit parametrisation of all these vectors is:

$$n^\mu = \frac{1}{\sqrt{2}}(1, 0, 0, -1), \quad \bar{n}^\mu = \frac{1}{\sqrt{2}}(1, 0, 0, 1), \quad R^\mu = -\frac{1}{\sqrt{2}}(0, 1, i, 0), \quad L^\mu = -\frac{1}{\sqrt{2}}(0, 1, -i, 0). \quad (1)$$

basic definitions):

$$\begin{aligned}\hat{F}_{q \leftarrow H}^{ij}(x, \xi, t) &= \int \frac{dz}{2\pi} e^{-ixP_+z} \left\langle P + \frac{\Delta}{2}, \Lambda' \left| \bar{q}^j \left( \frac{zn}{2} \right) \mathcal{W} \left[ \frac{zn}{2}, -\frac{zn}{2} \right] q^i \left( -\frac{zn}{2} \right) \right| P - \frac{\Delta}{2}, \Lambda \right\rangle, \\ \hat{F}_{g \leftarrow H}^{\mu\nu}(x, \xi, t) &= \int \frac{dz}{2\pi} \frac{e^{-ixP_+z}}{xP_+} \left\langle P + \frac{\Delta}{2}, \Lambda' \left| F_a^{\mu+} \left( \frac{zn}{2} \right) \mathcal{W}_{ab} \left[ \frac{zn}{2}, -\frac{zn}{2} \right] F_b^{\nu+} \left( -\frac{zn}{2} \right) \right| P - \frac{\Delta}{2}, \Lambda \right\rangle,\end{aligned}\tag{3}$$

where  $\xi = -\Delta_+/(2P_+)$ ,  $t = \Delta^2$ , and  $\mathcal{W}$  is the Wilson line defined as:

$$\mathcal{W}[yn, wn] = \mathbb{P} \exp \left\{ -ig(w - y)n^\nu T^c \int_0^1 ds A_\nu^c(swn + (1-s)yn) \right\},\tag{4}$$

where  $\mathbb{P}$  denotes the path ordering. The representation of the color-group generators  $T^c$  is the fundamental one in the quark case and the adjoint one in the gluon case. In the hadronic states,  $\Lambda$  and  $\Lambda'$  denote the helicity states of the incoming and outgoing hadron  $H$ , respectively. The relation between the spin vector  $S$  and the helicity  $\Lambda$  for a state of momentum  $p$  and mass  $M$  is given by:

$$S^\mu = \Lambda \frac{p_+ \bar{n}^\mu - p_- n^\mu}{M} - S_R L^\mu - S_L R^\mu.\tag{5}$$

At twist-2, three relevant projections are to be considered for both quarks and gluons: unpolarised, longitudinally polarised, and transversely (quark)/circularly (gluon) polarised. For the quark operator, the three cases are projected out as follows:

$$\hat{F}_{q \leftarrow H}^{[\Gamma]}(x, \xi, t) = \frac{1}{2} \text{Tr} \left[ \hat{F}_{q \leftarrow H}(x, \xi, t) \Gamma \right],\tag{6}$$

with:

$$\Gamma \in \{\not{1}, \not{5}, \not{5}\gamma_5, in_\beta \sigma^{\alpha\beta} \gamma_5\}.\tag{7}$$

In the gluon case, the projection is instead defined as:

$$\hat{F}_{g \leftarrow H}^{[\Gamma]}(x, \xi, t) = \Gamma_{\mu\nu} \hat{F}_{g \leftarrow H}^{\mu\nu}(x, \xi, t),\tag{8}$$

where the tensor  $\Gamma^{\mu\nu}$  is to be selected amongst the following structures:

$$\Gamma^{\mu\nu} \in \{-g_T^{\mu\nu} \equiv -(g^{\mu\nu} - n^\mu \bar{n}^\nu - \bar{n}^\mu n^\nu), -i\varepsilon_T^{\mu\nu} \equiv -i\varepsilon^{\alpha\beta\mu\nu} \bar{n}_\alpha n_\beta, -R^\mu R^\nu - L^\mu L^\nu\},\tag{9}$$

where we use the convention  $\varepsilon_T^{12} \equiv \bar{n}_\alpha n_\beta \varepsilon^{\alpha\beta 12} = +1$ .

The evolution kernels do not depend on the specific external states and therefore they are independent of how the correlators  $\hat{F}_{f \leftarrow H}$  are parametrised in terms of the single scalar GPDs. In principle, one could study the evolution equations in position space [48], where the independence of the external states is made transparent. This observation also implies that evolution equations for transition GPDs [9, 49] are identical to those for standard (flavour diagonal) GPDs.

The goal of this work is the evaluation of the one-loop (leading-order (LO)) evolution kernels in momentum space for all of the three twist-2 GPD correlators introduced above. Although these quantities are already known in the literature,<sup>†</sup> we aim to achieve an efficient numerical implementation and to lay the foundations for a systematic Feynman-graph approach to the computation. For this reason, we choose to work in light-cone gauge, which allows us to consider a significantly smaller number of diagrams. The light-cone gauge is obtained by enforcing the following condition on the gluon field:

$$A_+^c = 0.\tag{10}$$

It is well known that in light-cone gauges the condition above is not enough to completely fix the gauge [50]. Indeed, the transverse components of the gauge field at light-cone infinity are left

<sup>†</sup>For example, a list of all relevant one-loop kernels in position space and their transformation in momentum space can be found in Ref. [48].

unconstrained by Eq. (10). However, in the context of GPDs, the specific boundary condition on these transverse components is irrelevant. Indeed, the gauge link (Wilson line) runs along the light-cone direction and all operators are compact, thus shielding the GPDs from being sensitive to the boundary conditions at light-cone infinity.

A complication of working in light-cone gauge is that the gluon propagator has a more convoluted structure that reads:

$$\mathcal{D}^{\mu\nu}(k) = \frac{id^{\mu\nu}(k)}{k^2 + i0}, \quad d^{\mu\nu}(k) = -g^{\mu\nu} + \frac{k^\mu n^\nu + k^\nu n^\mu}{(nk)_{\text{reg}}}. \quad (11)$$

The subscript “reg.” indicates that the linear propagator  $(nk)^{-1}$ , which gives rise to the so-called rapidity divergences, has to be regularised. These spurious divergences, which are present in single diagrams, cancel out when summing over all diagrams, so that the regulator can eventually be safely removed. However, at one-loop the cancellation of the rapidity divergences is apparent and we find it unnecessary to specify a particular regularisation procedure.

The GPD correlators defined in Eq. (3) require UV renormalisation. Using dimensional regularisation in  $d = 4 - 2\varepsilon$  dimensions and the  $\overline{\text{MS}}$  renormalisation scheme, GPDs are renormalised in a multiplicative fashion by means of a set of renormalisation constants  $Z$  as follows:

$$F_{f \leftarrow H}^{[\Gamma]}(x, \xi, t; \mu) = \sum_{f'} \int_{-1}^1 \frac{dy}{|y|} Z_{f/f'}^{[\Gamma]} \left( \frac{x}{y}, \frac{\xi}{x}, \varepsilon, \alpha_s \right) \hat{F}_{f' \leftarrow H}^{[\Gamma]}(x, \xi, t; \varepsilon), \quad \Gamma = U, L, T, \quad (12)$$

where  $U$ ,  $L$ , and  $T$  stand for unpolarised, longitudinally polarised and transversely/circularly polarised projections, respectively.<sup>‡</sup> In addition, the sums over  $f'$  and/or  $f''$  run over active partons. The corresponding evolution equations for the renormalised GPDs take the general form [44]:

$$\frac{\partial F_{f \leftarrow H}^{[\Gamma]}(x, \xi, t; \mu)}{\partial \ln \mu^2} = \sum_{f'} \int_{-1}^1 \frac{dz}{|z|} \mathcal{P}_{f/f'}^{[\Gamma]} \left( \frac{x}{z}, \frac{\xi}{x}, \alpha_s(\mu) \right) F_{f' \leftarrow H}^{[\Gamma]}(z, \xi, t; \mu). \quad (13)$$

The evolution kernel  $\mathcal{P}$  are related to the renormalisation constants as:

$$\mathcal{P}_{f/f'}^{[\Gamma]} \left( \frac{x}{z}, \frac{\xi}{x}, \alpha_s(\mu) \right) = \lim_{\varepsilon \rightarrow 0} \sum_{f''} \int_{-1}^1 \frac{dy}{|y|} \left[ \frac{\partial}{\partial \ln \mu^2} Z_{f/f''}^{[\Gamma]} \left( \frac{x}{y}, \frac{\xi}{x}, \alpha_s, \varepsilon \right) \right] \left( Z_{f''/f'}^{[\Gamma]} \right)^{-1} \left( \frac{y}{z}, \frac{\xi}{y}, \alpha_s, \varepsilon \right). \quad (14)$$

The  $\overline{\text{MS}}$  renormalisation constants  $Z$  can depend on the renormalisation scale  $\mu$  only through the strong coupling  $\alpha_s$ . Therefore, defining  $a_s = \alpha_s/(4\pi)$ , we have that:

$$\begin{aligned} \frac{\partial}{\partial \ln \mu^2} Z_{f/f''}^{[\Gamma]} \left( \frac{x}{y}, \frac{\xi}{x}, \alpha_s, \varepsilon \right) &= \frac{\partial a_s}{\partial \ln \mu^2} \frac{\partial}{\partial a_s} Z_{f/f''}^{[\Gamma]} \left( \frac{x}{y}, \frac{\xi}{x}, \alpha_s, \varepsilon \right) \\ &= (-\varepsilon a_s + \beta(a_s)) \frac{\partial}{\partial a_s} \sum_{n=1}^n \sum_{p=1}^n \frac{a_s^n}{\varepsilon^p} Z_{f/f''}^{[\Gamma],[n,p]} \left( \frac{x}{y}, \frac{\xi}{x} \right) \\ &= \left( -\varepsilon + \frac{\beta(a_s)}{a_s} \right) \sum_{n=1}^n \sum_{p=1}^n \frac{n a_s^n}{\varepsilon^p} Z_{f/f''}^{[\Gamma],[n,p]} \left( \frac{x}{y}, \frac{\xi}{x} \right). \end{aligned} \quad (15)$$

Expanding the evolution kernel in powers of  $a_s$ :

$$\mathcal{P}_{f/f'}^{[\Gamma]} \left( \frac{x}{y}, \frac{\xi}{x}, \alpha_s \right) = a_s \sum_{n=0} a_s^n \mathcal{P}_{f/f'}^{[\Gamma],[n]} \left( \frac{x}{y}, \frac{\xi}{x} \right), \quad (16)$$

at LO we immediately obtain:

$$\mathcal{P}_{f/f'}^{[\Gamma],[0]} \left( \frac{x}{y}, \frac{\xi}{x} \right) = -Z_{f/f'}^{[\Gamma],[1,1]} \left( \frac{x}{y}, \frac{\xi}{x} \right). \quad (17)$$

<sup>‡</sup>Here and in the following we refer to transversely/circularly polarised GPDs with the index  $T$ , implicitly understanding transversely polarised quark GPDs and circularly polarised gluon GPDs.

Since the renormalisation constants are universal and independent of the external states, we can compute them perturbatively using the parton-in-parton GPDs, which are defined from the hadronic GPDs by replacing the external hadronic states with on-shell free partonic states [44]. Expanding the bare and renormalised parton-in-parton GPDs in powers of  $a_s$ :

$$\begin{aligned}\hat{F}_{f \leftarrow f'}^{[\Gamma]}(x, \xi, \varepsilon) &= \sum_{n=0} a_s^n \hat{F}_{f \leftarrow f'}^{[\Gamma], [n]}(x, \xi, \varepsilon), \\ F_{f \leftarrow f'}^{[\Gamma]}(x, \xi, \mu) &= \sum_{n=0} a_s^n F_{f \leftarrow f'}^{[\Gamma], [n]}(x, \xi, \mu),\end{aligned}\tag{18}$$

we can derive the renormalisation constants by plugging these expansions into Eq. (12) and requiring that the renormalised GPDs be finite order by order in  $a_s$ . This eventually produces the iterative set of equations:

$$F_{f \leftarrow f'}^{[\Gamma], [n]}(x, \xi, \mu) = \lim_{\varepsilon \rightarrow 0} \sum_{f''} \int_{-1}^1 \frac{dy}{|y|} \sum_{q=0}^n \sum_{k=1}^q \frac{1}{\varepsilon^k} Z_{f/f''}^{[\Gamma], [q, k]} \left( \frac{x}{y}, \frac{\xi}{x} \right) \hat{F}_{f'' \leftarrow f'}^{[\Gamma], [n-q]}(y, \xi, \varepsilon).\tag{19}$$

The coefficients  $Z_{f/f''}^{[\Gamma], [q, k]}$  are obtained by matching the UV divergences produced by the diagrammatic calculation of  $\hat{F}_{f'' \leftarrow f'}^{[\Gamma], [n-q]}$  in a way that  $F_{f \leftarrow f'}^{[\Gamma], [n]}$  are all finite.

### 3 Analytic results

As discussed above, the evolution kernels derive from the renormalisation of the parton-in-parton GPDs and only depend on the operator involved in their definition. As a consequence, the unpolarised GPDs  $H$  and  $E$  share the same evolution kernels, and so do the longitudinally polarised GPDs  $\tilde{H}$  and  $\tilde{E}$ , and the full set of transversely/circularly polarised GPDs  $H_T$ ,  $E_T$ ,  $\tilde{H}_T$ , and  $\tilde{E}_T$ .

The general form of the one-loop evolution kernels for each of these three classes of GPDs can be presented as follows:

$$\begin{aligned}\mathcal{P}_{i/k}^{[\Gamma], [0]} \left( x, \frac{\xi}{x} \right) &= \theta(1-x) \left[ \theta(x+\xi) p_{i/k}^{\Gamma} \left( x, \frac{\xi}{x} \right) + \theta(x-\xi) p_{i/k}^{\Gamma} \left( x, -\frac{\xi}{x} \right) \right] \\ &\quad + 2\delta_{ik} \delta(1-x) C_i \left[ K_i + \ln \left| 1 - \frac{\xi^2}{x^2} \right| - 2 \int_0^1 \frac{dz}{1-z} \right],\end{aligned}\tag{20}$$

where the  $\theta$  function is normalised such that  $\theta(0) = 1$ . The constants  $K_i$  and  $C_i$  are the same for all polarisations  $\Gamma$  and read:

$$K_q = \frac{3}{2}, \quad K_g = \frac{11}{6} - \frac{2n_f}{3} \frac{T_R}{C_A},\tag{21}$$

with  $C_q = C_F$  and  $C_g = C_A$ . Conversely, the functions  $p_{i/k}^{\Gamma}$  are different for each polarisation. Those associated with the unpolarised GPDs  $H$  and  $E$  have already been presented in Ref. [44], but we report them here for completeness:

$$p_{q/q}^U \left( x, \frac{\xi}{x} \right) = C_F \frac{(x+\xi)(1-x+2\xi)}{\xi(1+\xi)(1-x)},\tag{22}$$

$$p_{q/g}^U \left( x, \frac{\xi}{x} \right) = T_R \frac{(x+\xi)(1-2x+\xi)}{\xi(1+\xi)(1-\xi^2)},\tag{23}$$

$$p_{g/q}^U \left( x, \frac{\xi}{x} \right) = C_F \frac{(x+\xi)(2-x+\xi)}{x\xi(1+\xi)},\tag{24}$$

$$p_{g/g}^U \left( x, \frac{\xi}{x} \right) = -C_A \frac{x^2 - \xi^2}{x\xi(1-\xi^2)} \left[ 1 - \frac{2\xi}{1-x} - \frac{2(1+x^2)}{(x-\xi)(1+\xi)} \right].\tag{25}$$

In the longitudinally polarised case, instead, they read:

$$p_{q/q}^L \left( x, \frac{\xi}{x} \right) = C_F \frac{(x + \xi)(1 - x + 2\xi)}{\xi(1 + \xi)(1 - x)}, \quad (26)$$

$$p_{q/g}^L \left( x, \frac{\xi}{x} \right) = -T_R \frac{x + \xi}{\xi(1 + \xi)^2}, \quad (27)$$

$$p_{g/q}^L \left( x, \frac{\xi}{x} \right) = C_F \frac{(x + \xi)^2}{x\xi(1 + \xi)}, \quad (28)$$

$$p_{g/g}^L \left( x, \frac{\xi}{x} \right) = \frac{C_A(\xi + x)(-\xi^2(2\xi + 1) + \xi + (\xi - 3)x^2 + (\xi^2 + 3)x)}{(1 - \xi^2)\xi(1 + \xi)(1 - x)x}, \quad (29)$$

while in the transversely/circularly polarised case, they read:

$$p_{q/q}^T \left( x, \frac{\xi}{x} \right) = 2C_F \frac{x + \xi}{(1 + \xi)(1 - x)}, \quad (30)$$

$$p_{q/g}^T \left( x, \frac{\xi}{x} \right) = p_{g/q}^T \left( x, \frac{\xi}{x} \right) = 0, \quad (31)$$

$$p_{g/g}^T \left( x, \frac{\xi}{x} \right) = 2C_A \frac{(x + \xi)^2}{(1 + \xi)^2(1 - x)x}. \quad (32)$$

It is interesting to observe that in the transversely/circularly polarised case, due to the fact that the off-diagonal functions  $p_{q/g}^T$  and  $p_{g/q}^T$  are identically zero, transversely polarised quark GPDs and circularly polarised gluon GPD do not couple under evolution. More details on the computation of the functions above can be found in Appendix A.

Defining appropriate GPD combinations allows for a partial diagonalisation of the splitting matrix that is best suited for numerical implementations. At LO, these combinations are the non-singlet:

$$F^{[\Gamma],-} = \sum_{q=1}^{n_f} F_{q \leftarrow H}^{[\Gamma]} - F_{\bar{q} \leftarrow H}^{[\Gamma]}, \quad (33)$$

and the singlet:

$$F^{[\Gamma],+} = \begin{pmatrix} \sum_{q=1}^{n_f} F_{q \leftarrow H}^{[\Gamma]} + F_{\bar{q} \leftarrow H}^{[\Gamma]} \\ F_{g \leftarrow H}^{[\Gamma]} \end{pmatrix}, \quad (34)$$

where  $n_f$  is the number of active quark flavours and  $F_{i \leftarrow H}^{[U]} = H_{i \leftarrow H}, E_{i \leftarrow H}, F_{i \leftarrow H}^{[L]} = \tilde{H}_{i \leftarrow H}, \tilde{E}_{i \leftarrow H}, F_{i \leftarrow H}^{[T]} = H_{T,i \leftarrow H}, E_{T,i \leftarrow H}, \tilde{H}_{T,i \leftarrow H}, \tilde{E}_{T,i \leftarrow H}$  with  $i = q, g$ . In addition, we have defined anti-quark GPDs using the charge-conjugation symmetry relations:

$$F_{\bar{q} \leftarrow H}^{[\Gamma]}(x, \xi, t; \mu) = \mp F_{q \leftarrow H}^{[\Gamma]}(-x, \xi, t; \mu), \quad F_{g \leftarrow H}^{[\Gamma]}(x, \xi, t; \mu) = \mp F_{g \leftarrow H}^{[\Gamma]}(-x, \xi, t; \mu), \quad (35)$$

where the upper sign applies to the unpolarised and transversely/circularly polarised cases ( $\Gamma = U, T$ ), while the lower sign applies to the longitudinally polarised case ( $\Gamma = L$ ). Non-singlet and singlet GPD combinations obey their own decoupled evolution equations that at one loop read:

$$\frac{\partial F^{[\Gamma],\pm}(x, \xi, t; \mu)}{\partial \ln \mu^2} = \frac{\alpha_s(\mu)}{4\pi} \int_x^\infty \frac{dy}{y} \mathcal{P}^{[\Gamma],\pm,[0]}(y, \kappa) F^{[\Gamma],\pm} \left( \frac{x}{y}, \xi, t; \mu \right), \quad (36)$$

with  $\kappa = \xi/x$ . The evolution kernels  $\mathcal{P}$  can be decomposed as:

$$\mathcal{P}^{[\Gamma],\pm,[0]}(y, \kappa) = \theta(1 - y) \mathcal{P}_1^{[\Gamma],\pm,[0]}(y, \kappa) + \theta(\kappa - 1) \mathcal{P}_2^{[\Gamma],\pm,[0]}(y, \kappa), \quad (37)$$

with the non-singlet combinations given by:

$$\begin{aligned} \mathcal{P}_1^{[\Gamma],-, [0]}(y, \kappa) &= p_{q/q}^\Gamma(y, \kappa) + p_{q/q}^\Gamma(y, -\kappa) \\ &+ \delta(1 - y) 2C_q \left[ K_q - 2 \int_0^1 \frac{dz}{1 - z} - \ln |1 - \kappa^2| \right], \end{aligned} \quad (38)$$

$$\mathcal{P}_2^{[\Gamma],-, [0]}(y, \kappa) = -p_{q/q}^\Gamma(y, -\kappa) \pm p_{q/q}^\Gamma(-y, -\kappa),$$

and the singlet combinations given by:

$$\begin{aligned} \mathcal{P}_{1,ik}^{[\Gamma],+,[0]}(y,\kappa) &= p_{i/k}^{\Gamma}(y,\kappa) + p_{i/k}^{\Gamma}(y,-\kappa) \\ &+ \delta_{ik}\delta(1-y)2C_i \left[ K_i - 2 \int_0^1 \frac{dz}{1-z} - \ln|1-\kappa^2| \right], \end{aligned} \quad (39)$$

$$\mathcal{P}_{2,ik}^{[\Gamma],+,[0]}(y,\kappa) = -p_{i/k}^{\Gamma}(y,-\kappa) \mp p_{i/k}^{\Gamma}(-y,-\kappa),$$

where again the upper sign refers to unpolarised and transversely/circularly polarised distributions ( $\Gamma = U, T$ ), while the lower sign refers to the longitudinally polarised ones ( $\Gamma = L$ ). Explicit expressions for the one-loop non-polarised splitting kernels in this notation can be found in Ref. [44], but we report them here for completeness:

$$\begin{aligned} \left\{ \begin{aligned} \mathcal{P}_1^{[U],-,[0]}(y,\kappa) &= 2C_F \left\{ \left( \frac{2}{1-y} \right)_+ - \frac{1+y}{1-\kappa^2 y^2} + \delta(1-y) [K_q - \ln(|1-\kappa^2|)] \right\}, \\ \mathcal{P}_2^{[U],-,[0]}(y,\kappa) &= 2C_F \left[ \frac{1+(1+\kappa)y+(1+\kappa-\kappa^2)y^2}{(1+y)(1-\kappa^2 y^2)} - \left( \frac{1}{1-y} \right)_{++} \right], \end{aligned} \right. \\ \left\{ \begin{aligned} \mathcal{P}_{1,q\bar{q}}^{[U],+,[0]}(y,\kappa) &= \mathcal{P}_1^{-,[0]}(y,\kappa), \\ \mathcal{P}_{2,q\bar{q}}^{[U],+,[0]}(y,\kappa) &= 2C_F \left[ \frac{1+y+\kappa y+\kappa^3 y^2}{\kappa(1+y)(1-\kappa^2 y^2)} - \left( \frac{1}{1-y} \right)_{++} \right], \end{aligned} \right. \\ \left\{ \begin{aligned} \mathcal{P}_{1,qg}^{[U],+,[0]}(y,\kappa) &= 4n_f T_R \left[ \frac{y^2+(1-y)^2-\kappa^2 y^2}{(1-\kappa^2 y^2)^2} \right], \\ \mathcal{P}_{2,qg}^{[U],+,[0]}(y,\kappa) &= 4n_f T_R (1-\kappa) \left[ \frac{1-\kappa(\kappa+2)y^2}{\kappa(1-\kappa^2 y^2)^2} \right], \end{aligned} \right. \\ \left\{ \begin{aligned} \mathcal{P}_{1,g\bar{q}}^{[U],+,[0]}(y,\kappa) &= 2C_F \left[ \frac{1+(1-y)^2-\kappa^2 y^2}{y(1-\kappa^2 y^2)} \right], \\ \mathcal{P}_{2,g\bar{q}}^{[U],+,[0]}(y,\kappa) &= -2C_F \frac{(1-\kappa)^2}{\kappa(1-\kappa^2 y^2)}, \end{aligned} \right. \\ \left\{ \begin{aligned} \mathcal{P}_{1,gg}^{[U],+,[0]}(y,\kappa) &= 4C_A \left[ \left( \frac{1}{1-y} \right)_+ - \frac{1+\kappa^2 y}{1-\kappa^2 y^2} + \frac{1}{(1-\kappa^2 y^2)^2} \left( \frac{1-y}{y} + y(1-y) \right) \right. \\ &\quad \left. + \delta(1-y) \frac{K_g - \ln(|1-\kappa^2|)}{2} \right], \\ \mathcal{P}_{2,gg}^{[U],+,[0]}(y,\kappa) &= 2C_A \left[ \frac{2(1-\kappa)(1+y^2)}{(1-\kappa^2 y^2)^2} + \frac{\kappa^2(1+y)}{1-\kappa^2 y^2} + \frac{1-\kappa^2}{1-\kappa^2 y^2} \left( 2 - \frac{1}{\kappa} - \frac{1}{1+y} \right) - \left( \frac{1}{1-y} \right)_{++} \right]. \end{aligned} \right. \end{aligned} \quad (40)$$



The longitudinally polarised ones read:

$$\begin{cases}
\mathcal{P}_1^{[L],-,[0]}(y, \kappa) = 2C_F \left[ \left( \frac{2}{1-y} \right)_+ - \frac{1+y}{1-\kappa^2 y^2} + \delta(1-y) [K_q - \ln(|1-\kappa^2|)] \right], \\
\mathcal{P}_2^{[L],-,[0]}(y, \kappa) = 2C_F \left[ \frac{1+y+\kappa y+\kappa^3 y^2}{\kappa(1+y)(1-\kappa^2 y^2)} - \left( \frac{1}{1-y} \right)_{++} \right], \\
\mathcal{P}_{1,qq}^{[L],+,[0]}(y, \kappa) = \mathcal{P}_1^{[L],-,[0]}(y, \kappa), \\
\mathcal{P}_{2,qq}^{[L],+,[0]}(y, \kappa) = 2C_F \left[ \frac{1+(1+\kappa)y+(1+\kappa-\kappa^2)y^2}{(1+y)(1-\kappa^2 y^2)} - \left( \frac{1}{1-y} \right)_{++} \right], \\
\mathcal{P}_{1,qg}^{[L],+,[0]}(y, \kappa) = 4n_f T_R \left[ \frac{2y-1-\kappa^2 y^2}{(1-\kappa^2 y^2)^2} \right], \\
\mathcal{P}_{2,qg}^{[L],+,[0]}(y, \kappa) = -8n_f T_R (1-\kappa) \left[ \frac{y}{(1-\kappa^2 y^2)^2} \right], \\
\mathcal{P}_{1,gq}^{[L],+,[0]}(y, \kappa) = 2C_F \left[ \frac{2-y-\kappa^2 y}{1-\kappa^2 y^2} \right], \\
\mathcal{P}_{2,gq}^{[L],+,[0]}(y, \kappa) = 2C_F (1-\kappa)^2 \frac{y}{1-\kappa^2 y^2}, \\
\mathcal{P}_{1,gg}^{[L],+,[0]}(y, \kappa) = 4C_A \left[ \left( \frac{1}{1-y} \right)_+ + \frac{(1-\kappa^2 y)(1-2y-\kappa^2 y^2)}{(1-\kappa^2 y^2)^2} + \delta(1-y) \frac{K_g - \ln(|1-\kappa^2|)}{2} \right], \\
\mathcal{P}_{2,gg}^{[L],+,[0]}(y, \kappa) = 2C_A \left[ \frac{(2y+1)^2 - 4\kappa y(y+1) + 2\kappa^2 y - \kappa^4 y^3(y+2)}{(1+y)(1-\kappa^2 y^2)^2} - \left( \frac{1}{1-y} \right)_{++} \right]
\end{cases} \quad (41)$$

while the (non-zero) transversely polarised ones read:

$$\begin{cases}
\mathcal{P}_1^{[T],-,[0]}(y, \kappa) = 2C_F \left[ \left( \frac{2}{1-y} \right)_+ - \frac{2}{1-\kappa^2 y^2} + \delta(1-y) [K_q - \ln(|1-\kappa^2|)] \right], \\
\mathcal{P}_2^{[T],-,[0]}(y, \kappa) = 2C_F \left[ \frac{1+2\kappa y+\kappa(2-\kappa)y^2}{(1+y)(1-\kappa^2 y^2)} - \left( \frac{1}{1-y} \right)_{++} \right], \\
\mathcal{P}_{1,qq}^{[T],+,[0]}(y, \kappa) = \mathcal{P}_1^{[T],-,[0]}(y, \kappa), \\
\mathcal{P}_{2,qq}^{[T],+,[0]}(y, \kappa) = 2C_F \left[ \frac{1+2y+\kappa^2 y^2}{(1+y)(1-\kappa^2 y^2)} - \left( \frac{1}{1-y} \right)_{++} \right], \\
\mathcal{P}_{1,gq}^{[T],+,[0]}(y, \kappa) = 4C_A \left[ \left( \frac{1}{1-y} \right)_+ - \frac{(1-\kappa^2 y)(1+\kappa^2 y^2)}{(1-\kappa^2 y^2)^2} + \delta(1-y) \frac{K_g - \ln(|1-\kappa^2|)}{2} \right], \\
\mathcal{P}_{2,gq}^{[T],+,[0]}(y, \kappa) = 2C_A \left[ \frac{1+2y-4\kappa^2 y^2(\kappa-1)-\kappa^3 y^3(\kappa y+4)+2\kappa^2 y^3}{(1+y)(1-\kappa^2 y^2)^2} - \left( \frac{1}{1-y} \right)_{++} \right].
\end{cases} \quad (42)$$

The  $+$ -distribution (with round brackets) in the expressions above is defined as:

$$\int_x^1 dy \left( \frac{1}{1-y} \right)_+ f(y) = \int_x^1 dy \frac{f(y) - f(1)}{1-y} + f(1) \ln(1-x), \quad (43)$$

while the  $++$ -distribution instead is defined as:

$$\int_x^\infty dy \left( \frac{1}{1-y} \right)_{++} f(y) = \int_x^\infty \frac{dy}{1-y} \left[ f(y) - f(1) \left( 1 + \theta(y-1) \frac{1-y}{y} \right) \right] + f(1) \ln(1-x). \quad (44)$$

### 3.1 DGLAP limit

One of the fundamental requirements of the GPD evolution kernels is that, in the limit of vanishing  $\xi$ , the well-known DGLAP splitting functions have to be recovered. This limit amounts to taking  $\kappa \rightarrow 0$  and, given the decomposition in Eq. (37), it is such that  $\mathcal{P}_2^{[\Gamma],\pm,[0]}$  drops, leaving only the term proportional to  $\mathcal{P}_1^{[L],\pm,[0]}$ . The presence of  $\theta(1-y)$  in this term reduces the integral in the r.h.s. of Eq. (36) to a “standard” Mellin convolution which is precisely what enters the DGLAP evolution equations. What is left to verify is that  $\mathcal{P}_1^{[L],\pm,[0]}$  in the limit  $\kappa \rightarrow 0$  tend to the known one-loop DGLAP splitting functions. This has already been verified in Ref. [44] in the unpolarised case. Using Eq. (41), for the longitudinally polarised evolution kernels we find:

$$\begin{aligned} \lim_{\kappa \rightarrow 0} \mathcal{P}_1^{[L],-,[0]}(y, \kappa) &= \lim_{\kappa \rightarrow 0} \mathcal{P}_{1,q\bar{q}}^{[L],+,[0]}(y, \kappa) = 2C_F \left[ \left( \frac{2}{1-y} \right)_+ - (1+y) + \delta(1-y)K_q \right], \\ \lim_{\kappa \rightarrow 0} \mathcal{P}_{1,q\bar{q}}^{[L],+,[0]}(y, \kappa) &= 4n_f T_R (2y-1), \\ \lim_{\kappa \rightarrow 0} \mathcal{P}_{1,g\bar{g}}^{[L],+,[0]}(y, \kappa) &= 2C_F (2-y), \\ \lim_{\kappa \rightarrow 0} \mathcal{P}_{1,g\bar{g}}^{[L],+,[0]}(y, \kappa) &= 4C_A \left[ \left( \frac{1}{1-y} \right)_+ + 1 - 2y + \delta(1-y) \frac{K_g}{2} \right], \end{aligned} \quad (45)$$

that indeed coincide with the corresponding DGLAP splitting functions [51]. For the transversely polarised evolution kernels we take the limit for  $\kappa \rightarrow 0$  of Eq. (42) and find:

$$\begin{aligned} \lim_{\kappa \rightarrow 0} \mathcal{P}_1^{[T],-,[0]}(y, \kappa) &= \lim_{\kappa \rightarrow 0} \mathcal{P}_{1,q\bar{q}}^{[T],+,[0]}(y, \kappa) = 4C_F \left[ \left( \frac{1}{1-y} \right)_+ - 1 + \delta(1-y) \frac{K_q}{2} \right], \\ \lim_{\kappa \rightarrow 0} \mathcal{P}_{1,g\bar{g}}^{[T],+,[0]}(y, \kappa) &= 4C_A \left[ \left( \frac{1}{1-y} \right)_+ - 1 + \delta(1-y) \frac{K_g}{2} \right]. \end{aligned} \quad (46)$$

These expressions coincide with those from Refs. [52–54].<sup>§</sup>

### 3.2 ERBL limit

The evolution equations in Eq. (36) can be alternatively written in a form that resembles the ERBL equation [44, 55]:

$$\frac{\partial F^{[\Gamma],\pm}(x, \xi, t; \mu)}{\partial \ln \mu^2} = \frac{\alpha_s(\mu)}{4\pi} \int_{-1}^1 \frac{dy}{|\xi|} \mathbb{V}^{[\Gamma],\pm,[0]} \left( \frac{x}{\xi}, \frac{y}{\xi} \right) F^{[\Gamma],\pm}(y, \xi, t; \mu), \quad (47)$$

with:

$$\begin{aligned} \frac{1}{|\xi|} \mathbb{V}_{ik}^{[\Gamma],+,[0]} \left( \frac{x}{\xi}, \frac{y}{\xi} \right) &= \frac{1}{y} \left\{ [\theta(x-\xi)\theta(y-x) - \theta(-x-\xi)\theta(x-y)] \left[ p_{ik}^\Gamma \left( \frac{x}{y}, \frac{\xi}{x} \right) + p_{ik}^\Gamma \left( \frac{x}{y}, -\frac{\xi}{x} \right) \right] \right. \\ &\quad \left. + \theta(\xi-x)\theta(x+\xi) \left[ \theta(y-x)p_{ik}^\Gamma \left( \frac{x}{y}, \frac{\xi}{x} \right) - \theta(x-y)p_{ik}^\Gamma \left( \frac{x}{y}, -\frac{\xi}{x} \right) \right] \right\} \\ &\quad + \delta \left( 1 - \frac{x}{y} \right) \delta_{ik} 2C_i \left[ K_i + \int_\xi^x \frac{dz}{z-x} + \int_{-\xi}^x \frac{dz}{z-x} \right], \\ \frac{1}{|\xi|} \mathbb{V}_{ik}^{[\Gamma],-,[0]} \left( \frac{x}{\xi}, \frac{y}{\xi} \right) &= \frac{1}{|\xi|} \mathbb{V}_{q\bar{q}}^{[\Gamma],+,[0]} \left( \frac{x}{\xi}, \frac{y}{\xi} \right). \end{aligned} \quad (48)$$

<sup>§</sup>Note that in Eq. (13) of Ref. [54] the term proportional to the  $\delta$ -function is correct for the  $\Delta_T P_{q\bar{q}}^{(0)}$ , while it should be equal to  $K_g$  in the case of  $\Delta_L P_{g\bar{g}}^{(0)}$  (see Refs. [52, 53]).

Taking the  $\xi \rightarrow 1$  limit and performing the changes of variable  $x = 2v - 1$  and  $y = 2u - 1$ , the GPD evolution equations turn into ERBL evolution equations [55] for distribution amplitudes (DAs):

$$\frac{\partial \Phi^{[\Gamma],\pm}(v,t;\mu)}{\partial \ln \mu^2} = \frac{\alpha_s(\mu)}{4\pi} \int_0^1 du V^{[\Gamma],\pm,[0]}(v,u) \Phi^{[\Gamma],\pm}(u,t;\mu), \quad (49)$$

where the DAs  $\Phi^{[\Gamma],\pm}$  are related to the GPDs through the following identity:

$$\Phi^{[\Gamma],\pm}(v,t;\mu) = \lim_{\xi \rightarrow 1} F^{[\Gamma],\pm}(2v-1, \xi, t; \mu), \quad (50)$$

and the corresponding evolution kernels are defined as:

$$V^{[\Gamma],\pm,[0]}(v,u) = \lim_{\xi \rightarrow 1} \frac{1}{|\xi|} \mathbb{V}^{[\Gamma],\pm,[0]} \left( \frac{2v-1}{\xi}, \frac{2u-1}{\xi} \right). \quad (51)$$

Their explicit expressions in the unpolarised case are given by:

$$\begin{aligned} V^{[U],-,[0]}(v,u) &= V_{qq}^{+,[0]}(v,u) = -C_F \left[ \theta(u-v) \left( \frac{1-v}{u} - \frac{1}{u-v} \right) + \theta(v-u) \left( \frac{v}{1-u} - \frac{1}{v-u} \right) \right]_+, \\ V_{gg}^{[U],+,[0]}(v,u) &= -2n_f T_R \frac{2u-1}{2u(1-u)} \left[ \theta(u-v) \frac{v(u-2v+1)}{u} - \theta(v-u) \frac{(1-v)(2v-u)}{1-u} \right], \\ V_{gg}^{[U],+,[0]}(v,u) &= \frac{2C_F}{2v-1} \left[ \theta(u-v) \frac{v(2u-v)}{u} - \theta(v-u) \frac{(1-v)(v-2u+1)}{1-u} \right], \\ V_{gg}^{[U],+,[0]}(v,u) &= C_A \left[ \theta(u-v) \frac{(t^3(4u-2) - v^2(u+2)(2u-1) + v(2u((2u-3)u+2) - 1) + (u-1)u)}{(2v-1)(u-1)u^2} \right. \\ &\quad - \theta(v-u) \frac{(v^3(2-4u) + v^2(2u-1)(u+3) - v(2u-1)(2u^2+1) + ((4u-5)u+2)u)}{(2v-1)(u-1)^2u} \\ &\quad \left. + \left[ \frac{\theta(u-v)}{u-v} \right]_+ + \left[ \frac{\theta(v-u)}{v-u} \right]_+ \right] + \delta(v-u) C_A K_g. \end{aligned} \quad (52)$$

In Ref. [44], it was verified that, at least in the non-singlet case, these expressions coincide with those present in the literature. The longitudinally polarised expressions instead read:

$$\begin{aligned} V^{[L],-,[0]}(v,u) &= V_{qq}^{[L],+,[0]}(v,u) = -C_F \left[ \theta(u-v) \left( \frac{1-v}{u} - \frac{1}{u-v} \right) + \theta(v-u) \left( \frac{v}{1-u} - \frac{1}{v-u} \right) \right]_+, \\ V_{gg}^{[L],+,[0]}(v,u) &= -2n_f T_R \frac{2u-1}{2} \left[ \theta(u-v) \frac{v}{u^2} - \theta(v-u) \frac{1-v}{(1-u)^2} \right], \\ V_{gg}^{[L],+,[0]}(v,u) &= \frac{2C_F}{2v-1} \left[ \theta(u-v) \frac{v^2}{u} - \theta(v-u) \frac{(1-v)^2}{1-u} \right], \\ V_{gg}^{[L],+,[0]}(v,u) &= C_A \left[ \theta(u-v) \frac{(v^2((6u-7)u+2) - v(1-2u)^2 + (u-1)u)}{(2v-1)(u-1)u^2} \right. \\ &\quad - \theta(v-u) \frac{(v^2((5-6u)u-1) + v(8u^2-6u+1) + u(2-3u))}{(2v-1)(u-1)^2u} \\ &\quad \left. + \left[ \frac{\theta(u-v)}{u-v} \right]_+ + \left[ \frac{\theta(v-u)}{v-u} \right]_+ \right] + \delta(v-u) C_A K_g, \end{aligned} \quad (53)$$

while the transversely/circularly polarised ones are:

$$\begin{aligned}
V^{[T],-,[0]}(v,u) &= V_{qq}^{[T],+,[0]}(v,u) = C_F \left[ -\frac{\theta(u-v)}{u} - \frac{\theta(v-u)}{1-u} \right. \\
&\quad \left. + \left[ \frac{\theta(u-v)}{u-v} \right]_+ + \left[ \frac{\theta(v-u)}{v-u} \right]_+ \right] + \delta(v-u) C_F K_q, \\
V_{gg}^{[T],+,[0]}(v,u) &= C_A \left[ \frac{-2vu+v+u}{2v-1} \left( \frac{\theta(u-v)}{u^2} - \frac{\theta(v-u)}{(1-u)^2} \right) \right. \\
&\quad \left. + \left[ \frac{\theta(u-v)}{u-v} \right]_+ + \left[ \frac{\theta(v-u)}{v-u} \right]_+ \right] + \delta(v-u) C_A K_g.
\end{aligned} \tag{54}$$

The  $+$ -prescription in the expressions above, this time with square brackets, is defined differently from Eq. (43) and reads:

$$[f(v,u)]_+ = f(v,u) - \delta(u-v) \int_0^1 dv f(v,u). \tag{55}$$

To the best of our knowledge, the one-loop ERBL kernels for the full set of twist-2 distributions for both singlet and non-singlet combinations have not been presented anywhere.

### 3.3 Continuity at $x = \xi$ and spurious divergences

As it can be verified explicitly, all of the  $\mathcal{P}_2$  functions in Eqs. (40)-(42) are such that:

$$\mathcal{P}_2^{[\Gamma],\pm,[0]}(y,k) \propto (1-\kappa). \tag{56}$$

This property ensures that the r.h.s. of Eq. (36) is continuous at  $\kappa = 1$ , *i.e.* at the crossover point  $x = \xi$ . This is essential to ensure the continuity of GPDs at the crossover point.

Of course, GPD continuity also requires that the integral in the r.h.s. of Eq. (36) converges for all values of  $\kappa$ . However, as it can be seen from Eqs. (40)-(42), all of the single expressions for  $\mathcal{P}_1$  and  $\mathcal{P}_2$  are affected by a spurious pole at  $y = 1/\kappa$ . For  $\kappa \leq 1$ ,  $\mathcal{P}_2$  does not contribute to the evolution, while the pole of  $\mathcal{P}_1$ , that is to be integrated only up to  $y = 1$ , falls outside the integration region. As a consequence, the integral in this region converges. For  $\kappa > 1$ , both  $\mathcal{P}_1$  and  $\mathcal{P}_2$  contribute. As shown in Ref. [44] in the unpolarised case, it so happens that the coefficients of the poles at  $y = 1/\kappa$  of  $\mathcal{P}_1$  and  $\mathcal{P}_2$  are equal in absolute value but opposite in sign, such that the singularity cancels out leaving a finite result also for  $\kappa > 1$ .

In the following, we will prove that the same cancellation takes place also for the longitudinally and transversely/circularly polarised evolution kernels. Having ascertained that the cancellation needs to happen only for  $\kappa > 1$ , we concentrate on this region. For each evolution kernel we compute the following quantities:

$$\mathcal{L}^{[L]/[T],\pm} = \lim_{y \rightarrow \kappa^{-1}} \mathcal{P}_1^{[L]/[T],\pm,[0]}(y,\kappa) + \mathcal{P}_2^{[L]/[T],\pm,[0]}(y,\kappa), \tag{57}$$

and verify that they are finite. In the longitudinally polarised case we find:

$$\begin{aligned}
\mathcal{L}^{[L],-} &= C_F \frac{1 - 5\kappa^2}{\kappa(1 - \kappa^2)}, \\
\mathcal{L}_{qq}^{[L],+} &= C_F \frac{3\kappa^2 + 1}{\kappa^2 - 1}, \\
\mathcal{L}_{qg}^{[L],+} &= -n_f T_R, \\
\mathcal{L}_{gq}^{[L],+} &= 2C_F, \\
\mathcal{L}_{gg}^{[L],+} &= C_A \frac{1 - 5\kappa^2}{1 - \kappa^2},
\end{aligned} \tag{58}$$

while in the transversely/circularly polarised case, we have:

$$\begin{aligned}
\mathcal{L}^{[T],-} &= 2C_F \frac{\kappa^2 + 1}{\kappa^2 - 1}, \\
\mathcal{L}_{qq}^{[T],+} &= 4C_F \frac{\kappa}{\kappa^2 - 1}, \\
\mathcal{L}_{gg}^{[T],+} &= C_A \frac{\kappa(\kappa - 1)}{\kappa + 1},
\end{aligned} \tag{59}$$

that are indeed all finite for  $\kappa > 1$ , thus guaranteeing that the evolution at one loop leaves GPDs continuous at the crossover point  $x = \xi$ .

### 3.4 Sum rules

In this section, we discuss the sum rules. Specifically, it can be shown that polynomiality of GPDs implies some integral constraints of the evolution kernels. Ref. [44] discusses these constraints in the unpolarised case. In the longitudinally polarised case the conservation of the first moment leads to:<sup>¶</sup>

$$\int_0^1 dz \left[ \mathcal{P}_{1,ij}^{[L],+,[0]} \left( z, \frac{\xi}{yz} \right) + \frac{\xi}{y} \mathcal{P}_{2,ij}^{[L],+,[0]} \left( \frac{z\xi}{y}, \frac{1}{z} \right) \right] = \text{constant in } \xi, \tag{60}$$

where the independence of  $\xi$  also implies the independence of  $y$ . Indeed, we find:

$$\begin{aligned}
\int_0^1 dz \left[ \mathcal{P}_{1,qq}^{[L],+,[0]} \left( z, \frac{\xi}{yz} \right) + \frac{\xi}{y} \mathcal{P}_{2,qq}^{[L],+,[0]} \left( \frac{z\xi}{y}, \frac{1}{z} \right) \right] &= 0, \\
\int_0^1 dz \left[ \mathcal{P}_{1,qg}^{[L],+,[0]} \left( z, \frac{\xi}{yz} \right) + \frac{\xi}{y} \mathcal{P}_{2,qg}^{[L],+,[0]} \left( \frac{z\xi}{y}, \frac{1}{z} \right) \right] &= 0, \\
\int_0^1 dz \left[ \mathcal{P}_{1,gq}^{[L],+,[0]} \left( z, \frac{\xi}{yz} \right) + \frac{\xi}{y} \mathcal{P}_{2,gq}^{[L],+,[0]} \left( \frac{z\xi}{y}, \frac{1}{z} \right) \right] &= 3C_F, \\
\int_0^1 dz \left[ \mathcal{P}_{1,gg}^{[L],+,[0]} \left( z, \frac{\xi}{yz} \right) + \frac{\xi}{y} \mathcal{P}_{2,gg}^{[L],+,[0]} \left( \frac{z\xi}{y}, \frac{1}{z} \right) \right] &= \frac{11C_A - 4n_f T_R}{3}.
\end{aligned} \tag{61}$$

It is interesting to observe that, in the cases  $ij = qq, qg$ , the integrals above evaluate to zero. This implies that, at least at one-loop accuracy, the first moment the longitudinally polarised quark GPDs is independent of the scale  $\mu$  and can thus be identified with a physical observable.

---

<sup>¶</sup>Note that these constraints apply to all orders in perturbation theory and not only to the one-loop contribution.

This is indeed related to the anti-symmetric part of the energy-momentum tensor. It is known that the anti-symmetric form factor is related to the axial form factor that at one loop does not need renormalisation (see *e.g.* Refs. [21, 56, 57]). The same does not hold for the gluon part because at the level of the energy-momentum tensor no anti-symmetric and gauge invariant operator exists. Therefore, the third and fourth integrals in Eq. (61) are not forced to vanish.

The conservation of the longitudinally polarised second moment instead implies:

$$\int_0^1 dz z \left[ \mathcal{P}_1^{[L],-, [0]} \left( z, \frac{\xi}{yz} \right) + \frac{\xi^2}{y^2} \mathcal{P}_2^{[L],-, [0]} \left( \frac{z\xi}{y}, \frac{1}{z} \right) \right] = \text{constant in } \xi, \quad (62)$$

and indeed we find:

$$\int_0^1 dz z \left[ \mathcal{P}_1^{[L],-, [0]} \left( z, \frac{\xi}{yz} \right) + \frac{\xi^2}{y^2} \mathcal{P}_2^{[L],-, [0]} \left( \frac{z\xi}{y}, \frac{1}{z} \right) \right] = -\frac{8}{3} C_F. \quad (63)$$

In the transversely/circularly polarised case, and accounting for the fact that the  $qg$  and  $gq$  splitting kernels are identically zero, the sum rules imply that:

$$\begin{aligned} \int_0^1 dz \left[ \mathcal{P}_1^{[T],-, [0]} \left( z, \frac{\xi}{yz} \right) + \frac{\xi}{y} \mathcal{P}_2^{[T],-, [0]} \left( \frac{z\xi}{y}, \frac{1}{z} \right) \right] &= \text{constant in } \xi, \\ \int_0^1 dz z \left[ \mathcal{P}_{1,qg}^{[T],+, [0]} \left( z, \frac{\xi}{yz} \right) + \frac{\xi^2}{y^2} \mathcal{P}_{2,qg}^{[T],+, [0]} \left( \frac{z\xi}{y}, \frac{1}{z} \right) \right] &= \text{constant in } \xi, \\ \int_0^1 dz z \left[ \mathcal{P}_{1,gg}^{[T],+, [0]} \left( z, \frac{\xi}{yz} \right) + \frac{\xi^2}{y^2} \mathcal{P}_{2,gg}^{[T],+, [0]} \left( \frac{z\xi}{y}, \frac{1}{z} \right) \right] &= \text{constant in } \xi, \end{aligned} \quad (64)$$

and indeed we find:

$$\begin{aligned} \int_0^1 dz \left[ \mathcal{P}_1^{[T],-, [0]} \left( z, \frac{\xi}{yz} \right) + \frac{\xi}{y} \mathcal{P}_2^{[T],-, [0]} \left( \frac{z\xi}{y}, \frac{1}{z} \right) \right] &= -C_F, \\ \int_0^1 dz z \left[ \mathcal{P}_{1,qg}^{[T],+, [0]} \left( z, \frac{\xi}{yz} \right) + \frac{\xi^2}{y^2} \mathcal{P}_{2,qg}^{[T],+, [0]} \left( \frac{z\xi}{y}, \frac{1}{z} \right) \right] &= -3C_F, \\ \int_0^1 dz z \left[ \mathcal{P}_{1,gg}^{[T],+, [0]} \left( z, \frac{\xi}{yz} \right) + \frac{\xi^2}{y^2} \mathcal{P}_{2,gg}^{[T],+, [0]} \left( \frac{z\xi}{y}, \frac{1}{z} \right) \right] &= -\frac{7C_A + 4n_f T_R}{3}. \end{aligned} \quad (65)$$

The fulfilment of the sum rules provides a strong check of the correctness of the evolution kernels derived here.

### 3.5 Conservation of polynomiality

In this section, we prove analytically that GPD polynomiality is conserved by the evolution. The proof presented below is limited to the unpolarised non-singlet quark GPD, but a similar demonstration can be given also for the other cases. The polynomiality property reads:

$$\int_{-1}^1 dx x^{2n} F^{[U],-}(x, \xi, t; \mu) = \sum_{k=0}^n A_k^{(n)}(t, \mu) \xi^{2k}. \quad (66)$$

Using Eq. (47), one finds:

$$\sum_{k=0}^n \frac{\partial A_k^{(n)}(t, \mu)}{\partial \ln \mu^2} \xi^{2k} = \frac{\alpha_s(\mu)}{4\pi} \int_{-1}^1 dy \left[ \int_{-1}^1 \frac{dx}{|\xi|} x^{2n} \mathbb{V}^{[U],-, [0]} \left( \frac{x}{\xi}, \frac{y}{\xi} \right) \right] F^{[U],-}(y, \xi, t; \mu). \quad (67)$$

In order for this equality to be fulfilled, the following identity has to hold:

$$\int_{-1}^1 \frac{dx}{|\xi|} x^{2n} \mathbb{V}^{[U],-, [0]} \left( \frac{x}{\xi}, \frac{y}{\xi} \right) = \mathcal{V}_n^{[U],-, [0]} y^{2n}, \quad (68)$$

where  $\mathcal{V}_n^{[U],-, [0]}$  is a constant to be evaluated. The integral in the l.h.s. of the equation above can be computed using the results in Appendix C of Ref. [44], thus proving that the equality in Eq. (68) is indeed true with:

$$\mathcal{V}_n^{[U],-, [0]} = 2C_F \left[ \frac{3}{2} + \frac{1}{(n+1)(n+2)} - 2 \sum_{k=1}^{n+1} \frac{1}{k} \right]. \quad (69)$$

Interestingly, this allows us to derive evolution equations for the coefficients  $A_k^{(n)}$  that read:

$$\frac{\partial A_k^{(n)}(t, \mu)}{\partial \ln \mu^2} = \frac{\alpha_s(\mu)}{4\pi} \mathcal{V}_n^{[U],-, [0]} A_k^{(n)}(t, \mu), \quad (70)$$

and that admit the solution:

$$A_k^{(n)}(t, \mu) = \exp \left[ \frac{\mathcal{V}_n^{[U],-, [0]}}{4\pi} \int_{\mu_0}^{\mu} d \ln \mu'^2 \alpha_s(\mu') \right] A_k^{(n)}(t, \mu_0). \quad (71)$$

## 4 Numerical results

Having presented the expression for the evolution kernels in Sect. 3, we are now in a position to implement them in the numerical code **APFEL++** [46, 47].

To showcase the effect of the evolution, we have used as a set of initial-scale GPDs the realistic model of Refs. [58–60], referred to as Goloskokov-Kroll (GK) model, as implemented in **PARTONS** [40]. For the unpolarised evolution we selected the GPD  $H$ , in the longitudinally polarised case we instead used  $\tilde{H}$ , while in the transversely/circularly polarised case we used  $H_T$ . Since the GK model does not provide a circularly polarised gluon GPD, we used the unpolarised  $H_g$  as a proxy to test the evolution. Since the evolution of the circularly polarised gluon GPD is completely decoupled, no spurious effects are introduced in the evolution of the transversely polarised quark distributions that also evolve independently. GPDs are evolved from  $\mu_0 = 2$  GeV to  $\mu = 10$  GeV in the variable-flavour-number scheme (VFNS), *i.e.* allowing for heavy-flavour threshold crossing, with charm and bottom thresholds set to  $m_c = 2.1$  GeV and  $m_b = 4.75$  GeV, respectively.<sup>‡</sup> The strong coupling is consistently evolved at LO in the VFNS using  $\alpha_s(M_Z) = 0.118$  as a boundary condition. We set the value of the momentum transfer squared, that does not directly participate in the evolution, to  $t = -0.1$  GeV<sup>2</sup> throughout.

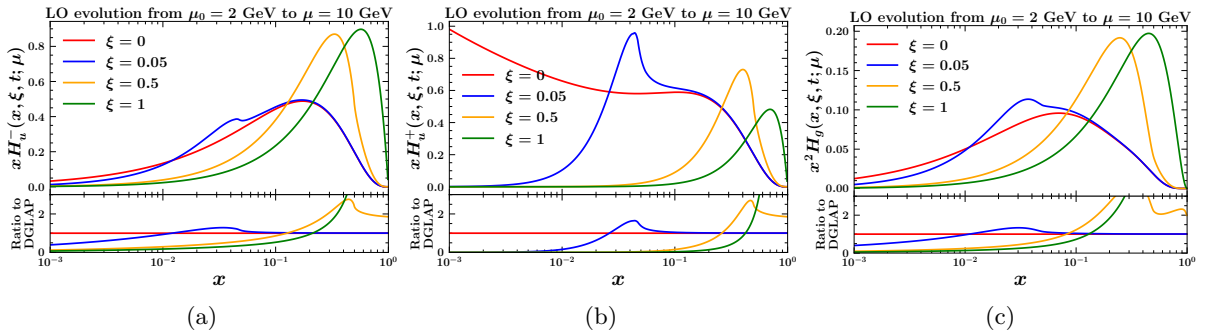


Figure 1: Evolution from  $\mu_0 = 2$  GeV to  $\mu = 10$  GeV for the unpolarised GPDs  $H$ . Panel (1a) shows the non-singlet up-quark GPD; panel (1b) shows the singlet up-quark GPD, and (1c) shows the gluon GPD.

Figs. 1, 2, and 3 show the effect on GPDs of unpolarised, longitudinally polarised, and transversely/circularly polarised evolutions, respectively. GPDs are displayed as functions of  $x$

<sup>‡</sup>The unusually large value of the charm threshold is due to the fact that the lowest available scale accessible to the GK model is  $\mu_0 = 2$  GeV [58–60]. However, at this scale, no distribution associated with the charm quark is provided. Therefore, we assumed  $n_f = 3$  active flavours at  $\mu_0$  which required setting  $m_c > \mu_0$ .

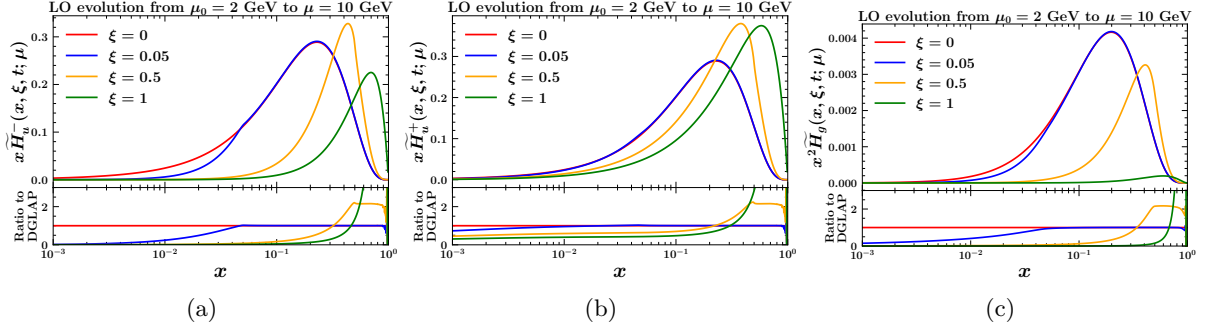


Figure 2: Same as Fig. 1 but for longitudinally polarised GPDs  $\tilde{H}$ .

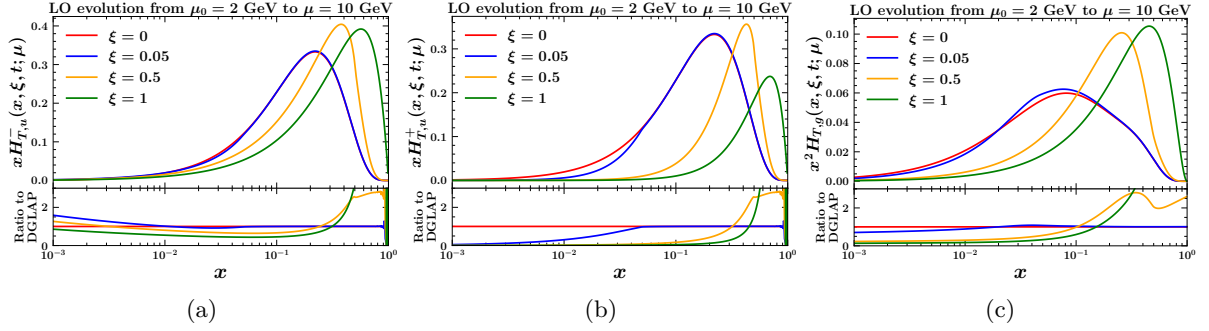


Figure 3: Same as Fig. 1 but for transversely/circularly polarised GPDs  $H_T$ .

for four different values of  $\xi$ , including the DGLAP ( $\xi = 0$ ) and ERBL ( $\xi = 1$ ) limits. The upper panels display the absolute distributions at the final scale  $\mu = 10$  GeV multiplied by a factor of  $x$  for the quark GPDs and  $x^2$  for the gluon GPDs for a better visualisation. The lower panels display their ratio to the corresponding distributions evolved using the DGLAP equations.

We first note that for all three cases, setting  $\xi = 0$  exactly reproduces the DGLAP evolution, as expected. For increasing values of  $\xi$ , the evolution gradually deviates from DGLAP for all considered distributions. The deviations are particularly pronounced for  $x \lesssim \xi$  where GPD evolution causes a strong slowdown of the evolution as compared to DGLAP. We also observe that GPDs at the crossover point  $x = \xi$  are continuous, as expected from the discussion in Sect. 3.3. However, they develop a cusp (discontinuity of the derivative in  $x$ ) that is a consequence of the fact that the evolution kernels are continuous but not smooth at  $x = \xi$ .

As discussed in Sect. 3.5, a crucial property of GPDs, that must be preserved by the evolution, is polynomiality. Figs. 4, 5, and 6 show the behaviour as functions of  $\xi$  of the first three even (left plots) and odd (right plots) moments of the up-quark distributions  $H$ ,  $\tilde{H}$ , and  $H_T$ , respectively. The bullets correspond to the values obtained by integrating numerically the evolved GPDs for different values of  $\xi$ , while the dashed lines show the fits using the expected polynomial laws in  $\xi$ . It is clear that in all cases, the expected behaviour is accurately reproduced. It is also interesting to observe that both even and odd first moments ( $n = 0$ ) for all polarisations are constant in  $\xi$ . In fact, this is the expected behaviour in all cases, except for the unpolarised even moment that would in principle admit a quadratic term in  $\xi$ . However, this contribution, often referred to as  $D$ -term, evolves independently from the rest of the GPD. Since the GK model does not include any  $D$ -term, the evolution does not generate it and it is thus absent at all scales, finally producing a constant first even moment also for the unpolarised GPD  $H$ .

Finally, in Figs. 7 and 8, we present a comparative analysis of the evolution of unpolarised and longitudinally polarised distributions between the code developed in Ref. [39], which we refer to as Vinnikov's code, and our implementation in **APFEL++**.\*\* To match the capabilities of Vinnikov's code, the comparison is performed without heavy-flavour threshold crossing. All other settings are consistent with those applied in the numerical results presented above.

\*\*Vinnikov's code does not include the implementation of transversely/circularly polarised evolution.



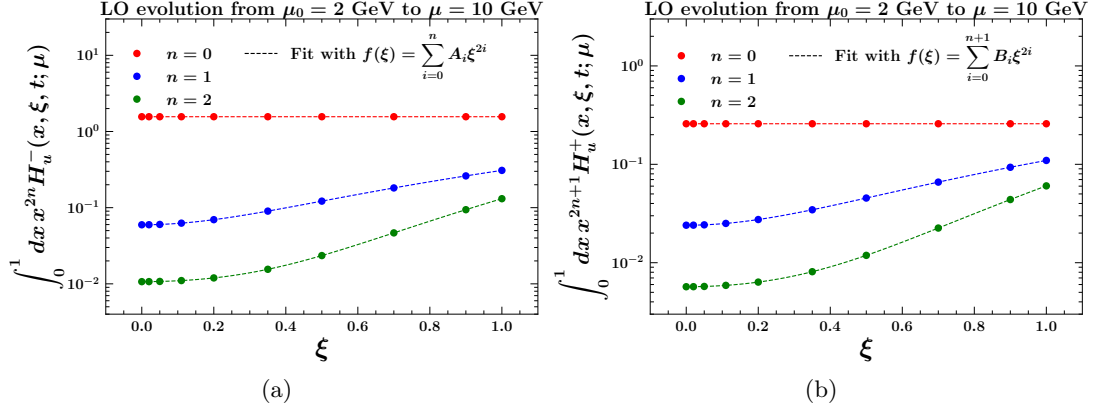


Figure 4: Effect of the evolution on the Mellin moments of the unpolarised up-quark GPD  $H$ . The bullets display the value of the moments computed numerically as integrals of the distributions, whereas the dashed lines show the fits to the bullets using the expected polynomial law. The left panel (4a) displays the first three even moments related to the non-singlet combination, while the right panel (4b) displays the first three odd moments that are instead related to the singlet combination.

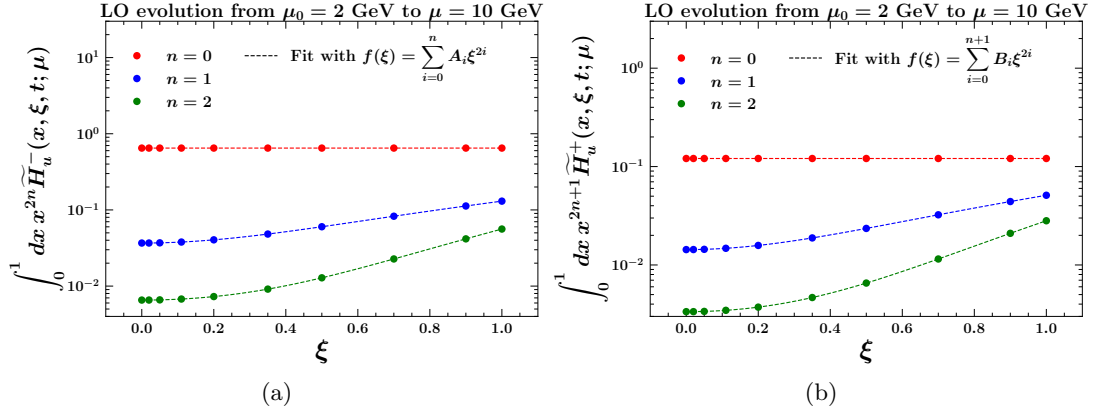


Figure 5: Same as Fig. 4 but for longitudinally polarised GPDs.

This comparison was already presented in Ref. [44] in the unpolarised case, where it was observed that, for small enough values of  $\xi$  ( $\xi \lesssim 0.6$ ), a generally good agreement between the two codes was achieved. However, for larger values of  $\xi$  ( $\xi \gtrsim 0.6$ ) a significant deterioration in the agreement was noted. Subsequently, we conducted a deeper investigation of this issue<sup>††</sup> that revealed that Vinnikov's code was indeed affected by a bug in the region  $\xi > 2/3$ . This issue is due to the way the  $x$ -space interpolation grid is constructed (see Eq. (6) of Ref. [39]). Specifically, the definition of the grid parameter  $\gamma$  in Eq. (6) of Ref. [39] guarantees that the constraints in Eqs. (7) and (9) are fulfilled only when  $\xi \leq 2/3$ , while they are broken for  $\xi > 2/3$ . Following the resolution of this issue,<sup>‡‡</sup> as illustrated in Figs. 7 and 8, a better agreement between APFEL++ and Vinnikov's code is found across a broad range of  $\xi$ , extending beyond  $\xi \simeq 0.6$ , for both unpolarised and longitudinally polarised evolutions.

In the unpolarised case (Fig. 7), the agreement generally remains at or below the percent level, with the only exception of the up-quark singlet distribution  $H_u^+$  at  $\xi = 1$ , which displays a larger departure of the order of 10-20% for small values of  $x$ . As far as the longitudinally polarised evolution is concerned (Fig. 8), the agreement between the two codes is excellent for  $\tilde{H}_u^+$ , while it tends to deteriorate at small  $x$  and large  $\xi$  for  $\tilde{H}_u^-$ . The disagreement is more pronounced for  $\tilde{H}_g$  where differences tend to increase with growing  $\xi$ , reaching the 40% level at

<sup>††</sup>Prompted by the referee's encouragement, we express our gratitude for this valuable suggestion.

<sup>‡‡</sup>The fix has been implemented in the current master branch of PARTONS.

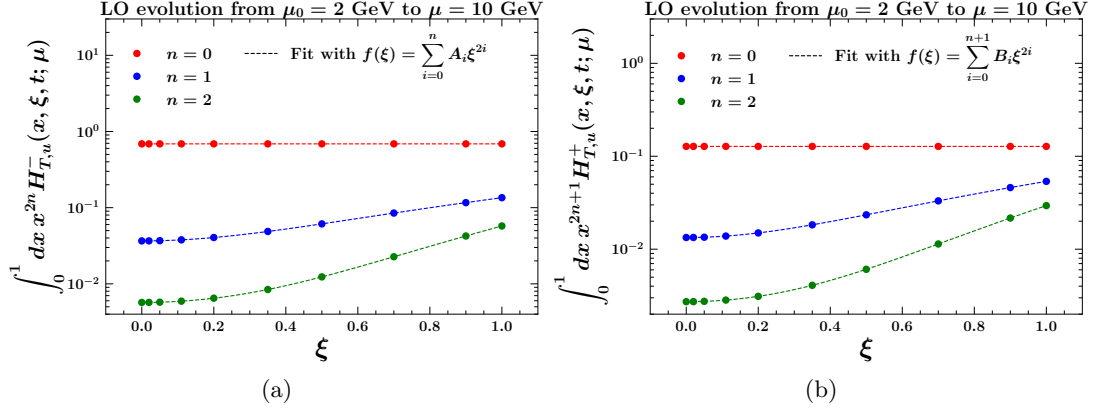


Figure 6: Same as Fig. 4 but for transversely/circularly polarised GPDs.

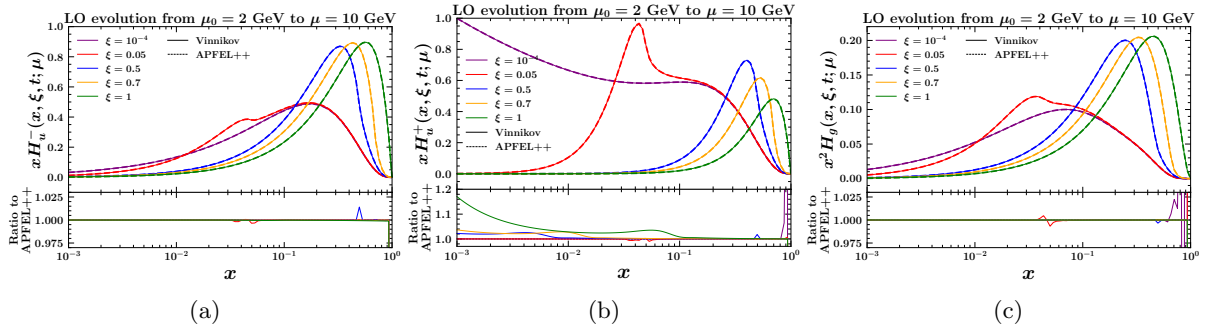


Figure 7: Comparison of the unpolarised evolution performed using the code of Ref. [39] (Vinnikov) and APFEL++. The panels (7a), (7b), and (7c) correspond to the non-singlet up-quark, singlet up-quark, and gluon GPDs, respectively.

$\xi = 1$  and small  $x$ . Unfortunately, we could not identify the origin of this residual discrepancy.

## 5 Conclusions

In this paper, we have revisited the evolution of all twist-2 GPDs, *i.e.* unpolarised, longitudinally polarised, and transversely/circularly polarised, at one-loop accuracy.

Our re-derivation of the evolution kernels closely follows that of Ref. [44], where the unpolarised evolution kernels were obtained, and extends it to the two remaining twist-2 polarisations. One of our main purposes is to obtain an efficient numerical implementation of the evolution of GPDs. This is achieved by recasting the GPD evolution equations in a form that resembles the DGLAP equations, which allowed us to exploit well-established numerical techniques to obtain

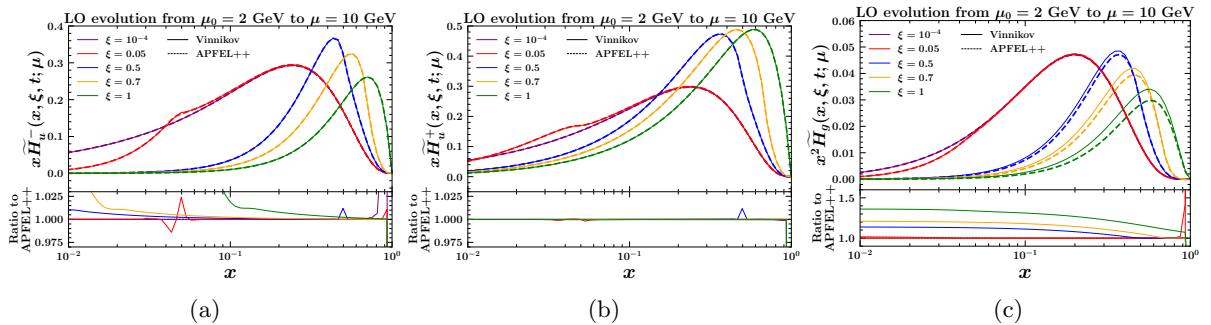


Figure 8: Same as Fig. 7 but for longitudinally polarised GPDs.

a solid implementation in the numerical code **APFEL++** [46, 47]. The computation is performed following a Feynman-graph approach in momentum space using the light-cone gauge (see Appendix A), paving the way for the extraction of the two-loop evolution kernels along the same lines of Ref. [61]. This will eventually allow us to achieve GPD evolution at next-to-leading order accuracy that, with the advent of the Electron-Ion Collider [24], will soon become a necessary ingredient for accurate phenomenology.

We have performed a number of analytic checks of the expressions obtained for the evolution kernels. Specifically, we have verified the correctness of the DGLAP ( $\xi \rightarrow 0$ ) and ERBL ( $\xi \rightarrow 1$ ) limits, ensured that the evolution does not cause any discontinuity of the GPDs at  $x = \xi$ , and proven that the kernels preserve polynomiality. Finally, we have thoroughly checked our numerical implementation of the evolution using as a set of initial-scale GPDs the realistic GK model [58–60] as provided by **PARTONS** [40]. We showed that the DGLAP limit is accurately recovered for all polarisations and that polynomiality is conserved upon evolution. Our implementation was also compared against an independent code (Vinnikov’s code [39]), revealing a generally good agreement.

## Acknowledgements

We thank P. Sznajder for helping us spot a bug in the code of Ref. [39]. This project is partially supported in part by the State Agency for Research of the Spanish Ministry of Science and Innovation through the grants PID2019-106080GB-C21, PCI2022-132984, PID2022-136510NB-C31, PID2022-136510NB-C33 and CNS2022-135186, by the Basque Government through the grant IT1628-22, as well as by the European Union Horizon 2020 research and innovation program under grant agreement Num. 824093 (STRONG-2020). OdR is supported by the MIU (Ministerio de Universidades, Spain) fellowship FPU20/03110. SR is supported by the Deutsche Forschungsgemeinschaft (DFG, German Research Foundation) – grant number 409651613 (Research Unit FOR 2926), subproject 430915355.

## A GPD evolution kernel integrals

In this appendix, we give a pedagogical review of the calculation of the one-loop evolution kernels for all twist-2 polarisations. Specifically, we show how the set of functions  $p_{i/k}^\Gamma$  in Eq. (20) are obtained.

### A.1 Quark-in-quark GPD

Since we are working in light-cone gauge, we can avoid considering gluons attaching to the Wilson line. Also, as the evolution kernels do not depend on  $\Delta_T^\mu$ , we can substitute in Eq. (3)  $|P - \Delta/2\rangle \rightarrow |(1 + \xi)P\rangle_i$  and  $\langle P + \Delta/2| \rightarrow {}_i\langle(1 - \xi)P|$ , with  $i = q, g$ . Hence, we rewrite the bare quark-in-quark GPD with interacting fields as follows:

$$\hat{F}_{q \leftarrow q}^{[\Gamma]}(x, \xi, \varepsilon) = \frac{1}{2N_c} \int \frac{dz}{2\pi} e^{-ixP_+z} \left\langle (1 - \xi)P \left| \bar{q}^j \left( \frac{z}{2} \right) \Gamma_{ji} q^i \left( -\frac{z}{2} \right) \right| (1 + \xi)P \right\rangle_q. \quad (72)$$

Before moving to the computation of the one-loop graphs, it is instructive to compute the tree-level graph first (Fig. 9).

In the absence of interactions, the quark fields can directly act on the momentum and spin partonic eigenstates, so that:

$$\begin{aligned} F_{q \leftarrow q}^{[\Gamma], [0]}(x, \xi) &= \frac{1}{4N_c} \int \frac{dz}{2\pi} e^{i(1-x)P_+z} \delta_{aa'} \bar{u}_{s', j}((1 - \xi)P) \Gamma_{ji} u_{s, i}((1 + \xi)P) \Lambda_{ss'}^{[\Gamma]} \\ &= \frac{1}{4} \int \frac{dz}{2\pi} e^{i(1-x)P_+z} \text{Tr} \left[ \Gamma u_s((1 + \xi)P) \Lambda_{ss'}^{[\Gamma]} \bar{u}_{s'}((1 - \xi)P) \right] \\ &= \frac{1}{4} \int \frac{dz}{2\pi} e^{i(1-x)P_+z} \sqrt{1 - \xi^2} \text{Tr} \left[ \Gamma \Lambda^{[\Gamma]} \right]. \end{aligned} \quad (73)$$

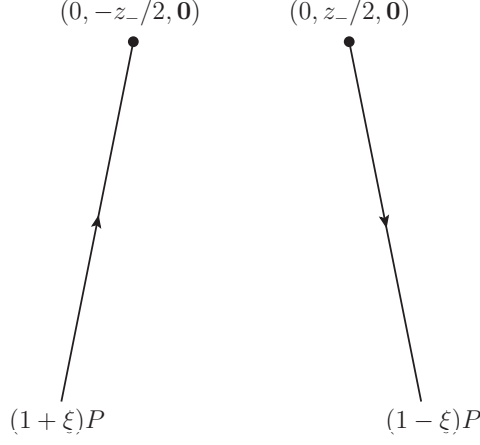


Figure 9: Leading-order diagram contributing to the quark-in-quark GPDs.

where  $\Lambda_{ss'}^{[\Gamma]}$  is a projector introduced for convenience to select the desired polarisation of the external quark state. The three relevant polarisations (unpolarised, longitudinally polarised, and transversely polarised) produce the following outcome when summed over the spin states  $s$  and  $s'$ :  $\Lambda^{[\Gamma]} = u_s(P) \Lambda_{ss'}^{[\Gamma]} \bar{u}_{s'}(P) \in \{\not{P}, \not{P}\gamma_5, i\sigma^{\sigma\rho}P_\rho\gamma_5\}$ , respectively. The trace in Eq. (73) is easily computed yielding:

$$F_{q\leftarrow q}^{[U],[0]}(x, \xi) = F_{q\leftarrow q}^{[L],[0]}(x, \xi) = F_{q\leftarrow q}^{[T],[0]}(x, \xi) = \sqrt{1 - \xi^2} \delta(1 - x). \quad (74)$$

As expected, in the limit  $\xi \rightarrow 0$ , the leading-order quark-in-quark PDFs are recovered. However, it is also interesting to observe that in the limit  $\xi \rightarrow 1$  the leading-order GPD vanishes. This is indeed the correct behavior because the limit  $\xi \rightarrow 1$  corresponds to a distribution amplitude that encodes the creation of meson bound state out of a pair of incoming quark-antiquark. Of course, this cannot happen without any interaction between the quark and the anti-quark. Therefore, the leading-order graph has to vanish.

Now, we can use the same procedure to compute the one-loop correction to the quark-in-quark GPDs whose relevant diagram is displayed in Fig. 10.

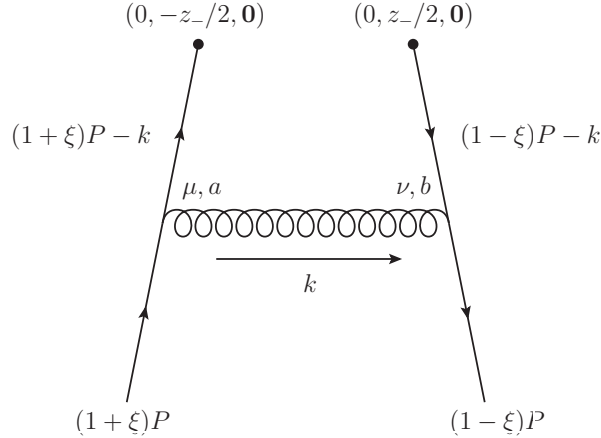


Figure 10: One-loop diagram contributing to the quark-in-quark GPD.

The integral to compute is:

$$a_s \hat{F}_{q\leftarrow q}^{[\Gamma],[1]}(x, \xi, \varepsilon) = \sqrt{1 - \xi^2} \int_{-\infty}^{\infty} \frac{dz}{2\pi} e^{i(1-x)P_+z} \text{Tr} \left[ R_{qq}^{[\Gamma]}(z, \xi, \varepsilon) \Lambda^{[\Gamma]} \right], \quad (75)$$

with

$$R_{qq}^{[\Gamma]}(z, \xi, \varepsilon) = i a_s C_F \int \frac{d^{4-2\epsilon}k}{(2\pi)^{2-2\epsilon}} e^{-ik_+z} \frac{\gamma^\mu [(1 + \xi)\not{P} - \not{k}] \Gamma [(1 - \xi)\not{P} - \not{k}] \gamma^\nu \mathcal{D}_{\mu\nu}(k)}{[(1 + \xi)P - k]^2 + i\varepsilon [((1 - \xi)P - k)^2 + i\varepsilon]}. \quad (76)$$

This integral will give different results depending on the relative position of  $x$  and  $\xi$ . In particular, the region  $x < \xi$  corresponds to the ERBL region, while  $x > \xi$  corresponds to the DGLAP region. The functions  $p_{q/q}^\Gamma$  can then be obtained by extracting the  $\overline{\text{MS}}$  UV pole part of this integral in these regions as shown in the Appendix of Ref. [44].

## A.2 Gluon-in-gluon GPD

We now consider the gluon-in-gluon GPD whose operator definition in light-cone gauge reduces to:

$$\hat{F}_{g \leftarrow g}^{[\Gamma]}(x, \xi, \varepsilon) = -\frac{P_+(x^2 - \xi^2)}{2(N_c^2 - 1)x} \int \frac{dy}{2\pi} e^{-ixp+y} \left\langle (1-\xi)P \left| A_a^\mu \left( \frac{z}{2} \right) \Gamma_{\mu\nu} A_a^\nu \left( -\frac{z}{2} \right) \right| (1+\xi)P \right\rangle_g. \quad (77)$$

The leading-order contribution is obtained using free fields and plugging in the Lorentz structures  $\Gamma_{\mu\nu}$  given in Eq. (9). The result is:

$$F_{g \leftarrow g}^{[U],[0]}(x, \xi) = F_{g \leftarrow g}^{[L],[0]}(x, \xi) = F_{g \leftarrow g}^{[T],[0]}(x, \xi) = (1 - \xi^2) \delta(1 - x). \quad (78)$$

The next-to-leading order correction is obtained considering the diagrams in Fig. 11.

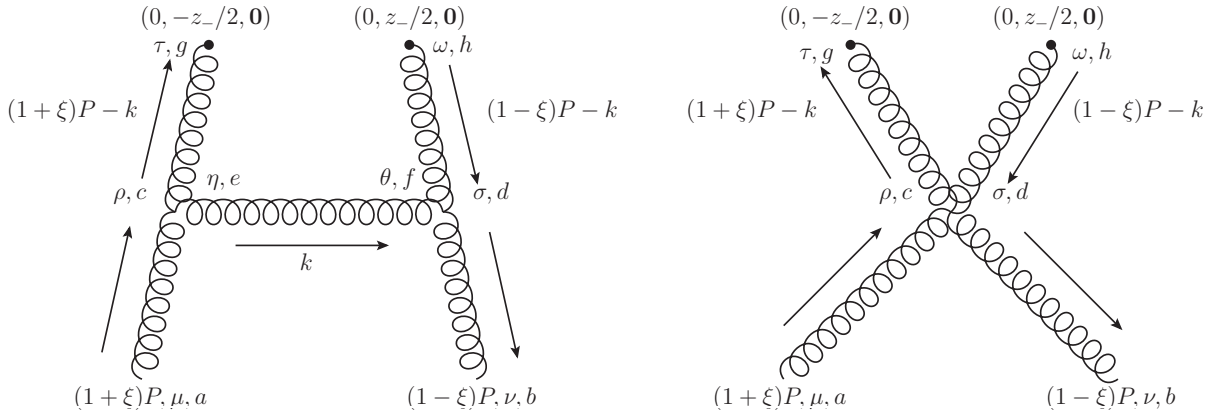


Figure 11: One-loop diagrams contributing to the gluon-in-gluon GPD.

The integral to compute for the left diagram is:

$$a_s \hat{F}_{g \leftarrow g, 3g}^{[\Gamma],[1]}(x, \xi, \varepsilon) = -\frac{P_+(x^2 - \xi^2)}{2(N_c^2 - 1)x} \int_{-\infty}^{\infty} \frac{dz}{2\pi} e^{i(1-x)P_+z} R_{3g}^{[\Gamma]}(z, \xi, \varepsilon), \quad (79)$$

with:

$$R_{3g}^{[\Gamma]}(z, \xi) = -4i a_s f^{ace} f^{eca} \int \frac{d^{4-2\epsilon}k}{(2\pi)^{2-2\epsilon}} e^{-ik_+z} V_{\mu\rho\eta}((1+\xi)P, -(1+\xi)P+k, -k) \\ \times \frac{\Lambda^{[\Gamma]\mu\nu} d^{\rho\tau}((1+\xi)P-k) d^{\eta\theta}(k) d^{\omega\sigma}((1-\xi)P-k) \Gamma_{\tau\omega}}{[((1+\xi)P-k)^2 + i\varepsilon][k^2 + i\varepsilon][((1-\xi)P-k)^2 + i\varepsilon]} V_{\theta\sigma\nu}(k, (1-\xi)P-k, -(1-\xi)P), \quad (80)$$

where:

$$V^{\mu\nu\rho}(q, l, r) = -[g^{\mu\nu}(q-l)^\rho + g^{\nu\rho}(l-r)^\mu + g^{\rho\mu}(r-q)^\nu]. \quad (81)$$

Similarly to the quark-in-quark distribution, the projector  $\Lambda^{[\Gamma]\mu\nu}$  selects the relevant gluon polarisation according to:

$$\Lambda^{[\Gamma]\mu\nu} = e_{s'}^{*\mu}(P) \Lambda_{ss'}^{[\Gamma]} e_s^\nu(P), \quad (82)$$

where the tensor  $\Lambda^{[\Gamma]\mu\nu}$  is to be selected amongst the following Lorentz structures:

$$-d^{\mu\nu}(P), \quad -i\varepsilon_T^{\mu\nu}(P) \equiv -i \frac{\varepsilon^{\alpha\beta\mu\nu} P_\alpha n_\beta}{(nP)}, \quad -R^\mu R^\nu - L^\mu L^\nu, \quad (83)$$

for unpolarised, longitudinally polarised, and circularly polarised gluons, respectively.

The integral corresponding to the four-gluon-vertex diagram on the r.h.s. of Fig. 11 is:

$$a_s \hat{F}_{g \leftarrow g, 4g}^{[\Gamma], [1]}(x, \xi, \varepsilon) = -\frac{P_+(x^2 - \xi^2)}{2(N_c^2 - 1)x} \int_{-\infty}^{\infty} \frac{dz}{2\pi} e^{i(1-x)P_+z} R_{4g}^{[\Gamma]}(z, \xi), \quad (84)$$

with:

$$R_{4g}^{[\Gamma]}(z, \xi) = 4ia_s \int \frac{d^{4-2\epsilon}k}{(2\pi)^{2-2\epsilon}} e^{-ik_+z} \frac{d^{\rho\tau}((1+\xi)P - k)}{((1+\xi)P - k)^2 + i\varepsilon} \frac{d^{\omega\sigma}((1-\xi)P - k)}{((1-\xi)P - k)^2 + i\varepsilon} \Lambda^{[\Gamma]\mu\nu} W_{\mu\rho\sigma\nu}^{bggb} \Gamma_{\tau\omega}, \quad (85)$$

where  $W_{\mu\rho\sigma\nu}^{bggb}$  is the four-gluon-vertex Feynman rule given by:

$$W_{\mu\nu\rho\sigma}^{abcd} = f^{eab} f^{ecd} (g_{\mu\rho} g_{\nu\sigma} - g_{\mu\sigma} g_{\nu\rho}) + f^{eac} f^{ebd} (g_{\mu\nu} g_{\rho\sigma} - g_{\mu\sigma} g_{\nu\rho}) + f^{ead} f^{ebc} (g_{\mu\nu} g_{\rho\sigma} - g_{\mu\rho} g_{\nu\sigma}). \quad (86)$$

Extracting the UV pole part of these diagrams for the different polarisations leads to the functions  $p_{g/g}^\Gamma$  given in Eqs. (25), (29), and (32).

### A.3 Quark-in-gluon and gluon-in-quark GPDs

We now consider the off-diagonal quark-in-gluon and gluon-in-quark GPDs whose operator definitions are:

$$\begin{aligned} \hat{F}_{g \leftarrow q}^{[\Gamma]}(x, \xi, \varepsilon) &= \frac{1}{4(N_c^2 - 1)} \int \frac{dz}{2\pi} e^{-ixP_+z} \left\langle (1-\xi)P \left| \bar{q}^j \left( \frac{z}{2} \right) \Gamma_{ji} q^i \left( -\frac{z}{2} \right) \right| (1+\xi)P \right\rangle_g, \\ \hat{F}_{q \leftarrow g}^{[\Gamma]}(x, \xi, \varepsilon) &= -\frac{p_+(x^2 - \xi^2)}{2N_c x} \int \frac{dy}{2\pi} e^{-ixp_+y} \left\langle (1-\xi)P \left| A_a^\mu \left( \frac{z}{2} \right) \Gamma_{\mu\nu} A_a^\nu \left( -\frac{z}{2} \right) \right| (1+\xi)P \right\rangle_q. \end{aligned} \quad (87)$$

These GPDs have no tree-level contribution and the first non-vanishing contribution appears at  $\mathcal{O}(\alpha_s)$ . The corresponding diagrams are shown in Fig. 12.

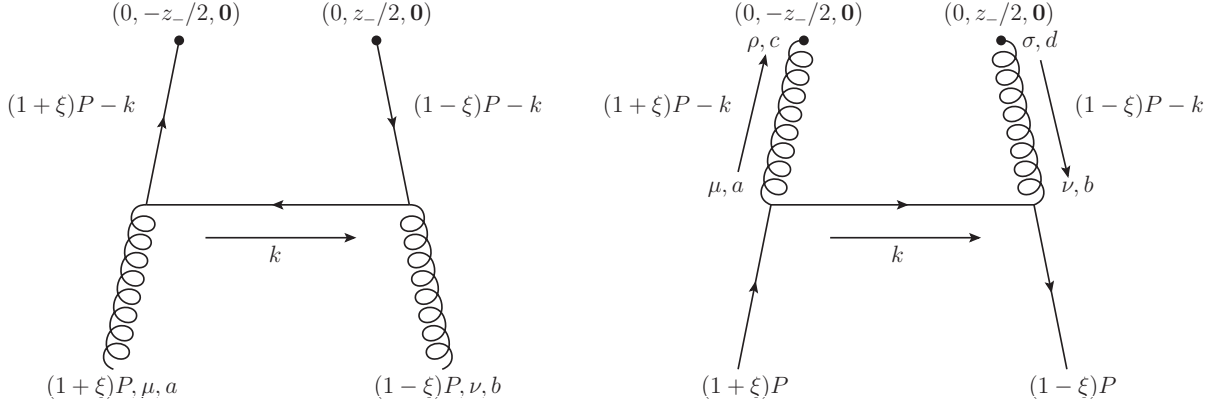


Figure 12: One-loop diagrams contributing to the quark-in-gluon (left) and the gluon-in-quark (right) GPDs.

The integral to be computed for the quark-in-gluon diagram is:

$$a_s \hat{F}_{g \leftarrow q}^{[\Gamma], [1]}(x, \xi, \varepsilon) = \int_{-\infty}^{\infty} \frac{dz}{2\pi} e^{i(1-x)P_+z} \text{Tr} \left[ R_{qg}^{[\Gamma]}(z, \xi, \varepsilon) \right], \quad (88)$$

where:

$$\begin{aligned} R_{qg}^{[\Gamma]}(z, \xi, \varepsilon) &= ia_s T_R \int \frac{d^{2-2\epsilon}k_T}{(2\pi)^{2-2\epsilon}} dk_+ dk_- e^{-ik_+z} \Lambda^{[\Gamma]\mu\nu} \frac{\not{k}}{k^2 + i\varepsilon} \gamma_\mu \\ &\quad \times \frac{((1+\xi)\not{P} - \not{k})}{((1+\xi)P - k)^2 + i\varepsilon} \Gamma \frac{(1-\xi)\not{P} - \not{k}}{((1-\xi)P - k)^2 + i\varepsilon} \gamma_\nu. \end{aligned} \quad (89)$$

While the one-loop gluon-in-quark diagram is computed as:

$$a_s \hat{F}_{q \leftarrow g}^{[\Gamma],[1]}(x, \xi, \varepsilon) = -\frac{P_+(x^2 - \xi^2)\sqrt{1 - \xi^2}}{2x} \int_{-\infty}^{\infty} \frac{dz}{2\pi} e^{i(1-x)P_+z} \text{Tr} \left[ R_{gq}^{[\Gamma]}(z, \xi, \varepsilon) \Lambda^{[\Gamma]} \right], \quad (90)$$

where:

$$R_{gq}^{[\Gamma]}(z, \xi, \varepsilon) = 4ia_s C_F \int \frac{d^{2-2\epsilon} \mathbf{k}_T}{(2\pi)^{2-2\epsilon}} dk_+ dk_- e^{-ik_+z} \gamma_\mu \frac{\not{k}}{k^2 + i\varepsilon} \times \frac{d^{\mu\rho}((1+\xi)P - k)}{((1+\xi)P - k)^2 + i\varepsilon} \Gamma^{\rho\sigma} \frac{d^{\sigma\nu}((1-\xi)P - k)}{((1-\xi)P - k)^2 + i\varepsilon} \gamma_\nu. \quad (91)$$

Once again, the UV pole part of these integrals allows us to obtain the functions  $p_{q/g}^\Gamma$  and  $p_{g/q}^\Gamma$ .

## References

- [1] D. Müller, D. Robaschik, B. Geyer, F. M. Dittes, and J. Hořejši, “Wave functions, evolution equations and evolution kernels from light ray operators of QCD,” *Fortsch. Phys.* **42** (1994) 101–141, [arXiv:hep-ph/9812448](#).
- [2] X.-D. Ji, “Gauge-Invariant Decomposition of Nucleon Spin,” *Phys. Rev. Lett.* **78** (1997) 610–613, [arXiv:hep-ph/9603249](#).
- [3] A. V. Radyushkin, “Scaling limit of deeply virtual Compton scattering,” *Phys. Lett. B* **380** (1996) 417–425, [arXiv:hep-ph/9604317](#).
- [4] A. V. Radyushkin, “Asymmetric gluon distributions and hard diffractive electroproduction,” *Phys. Lett. B* **385** (1996) 333–342, [arXiv:hep-ph/9605431](#).
- [5] X.-D. Ji, “Deeply virtual Compton scattering,” *Phys. Rev. D* **55** (1997) 7114–7125, [arXiv:hep-ph/9609381](#).
- [6] A. V. Radyushkin, “Nonforward parton distributions,” *Phys. Rev. D* **56** (1997) 5524–5557, [arXiv:hep-ph/9704207](#).
- [7] X.-D. Ji, “Off forward parton distributions,” *J. Phys. G* **24** (1998) 1181–1205, [arXiv:hep-ph/9807358](#).
- [8] M. Diehl, “Generalized parton distributions,” *Phys. Rept.* **388** (2003) 41–277, [arXiv:hep-ph/0307382](#).
- [9] A. V. Belitsky and A. V. Radyushkin, “Unraveling hadron structure with generalized parton distributions,” *Phys. Rept.* **418** (2005) 1–387, [arXiv:hep-ph/0504030](#).
- [10] S. Boffi and B. Pasquini, “Generalized parton distributions and the structure of the nucleon,” *Riv. Nuovo Cim.* **30** no. 9, (2007) 387–448, [arXiv:0711.2625 \[hep-ph\]](#).
- [11] K. Goeke, M. V. Polyakov, and M. Vanderhaeghen, “Hard exclusive reactions and the structure of hadrons,” *Prog. Part. Nucl. Phys.* **47** (2001) 401–515, [arXiv:hep-ph/0106012](#).
- [12] K. Kumericki, S. Liuti, and H. Moutarde, “GPD phenomenology and DVCS fitting: Entering the high-precision era,” *Eur. Phys. J. A* **52** no. 6, (2016) 157, [arXiv:1602.02763 \[hep-ph\]](#).
- [13] V. M. Braun, A. N. Manashov, S. Moch, and J. Schoenleber, “Two-loop coefficient function for DVCS: vector contributions,” *JHEP* **09** (2020) 117, [arXiv:2007.06348 \[hep-ph\]](#). [Erratum: JHEP 02, 115 (2022)].



- [14] V. M. Braun, Y. Ji, and J. Schoenleber, “Deeply Virtual Compton Scattering at Next-to-Next-to-Leading Order,” *Phys. Rev. Lett.* **129** no. 17, (2022) 172001, [arXiv:2207.06818 \[hep-ph\]](#).
- [15] V. Braun, A. Manashov, S.-O. Moch, and J. Schoenleber, “Vector and axial-vector coefficient functions for DVCS at NNLO,” *PoS LL2022* (2022) 074.
- [16] J. Schoenleber, “Resummation of threshold logarithms in deeply-virtual Compton scattering,” *JHEP* **02** (2023) 207, [arXiv:2209.09015 \[hep-ph\]](#).
- [17] Y. Ji and J. Schoenleber, “Two-loop coefficient functions in deeply virtual Compton scattering: flavor-singlet axial-vector and transversity case,” *JHEP* **01** (2024) 053, [arXiv:2310.05724 \[hep-ph\]](#).
- [18] M. Burkardt, “Impact parameter space interpretation for generalized parton distributions,” *Int. J. Mod. Phys. A* **18** (2003) 173–208, [arXiv:hep-ph/0207047](#).
- [19] M. V. Polyakov and P. Schweitzer, “Forces inside hadrons: pressure, surface tension, mechanical radius, and all that,” *Int. J. Mod. Phys. A* **33** no. 26, (2018) 1830025, [arXiv:1805.06596 \[hep-ph\]](#).
- [20] H. Dutrieux, C. Lorcé, H. Moutarde, P. Sznajder, A. Trawiński, and J. Wagner, “Phenomenological assessment of proton mechanical properties from deeply virtual Compton scattering,” *Eur. Phys. J. C* **81** no. 4, (2021) 300, [arXiv:2101.03855 \[hep-ph\]](#).
- [21] A. Freese, A. Metz, B. Pasquini, and S. Rodini, “The gravitational form factors of the electron in quantum electrodynamics,” *Phys. Lett. B* **839** (2023) 137768, [arXiv:2212.12197 \[hep-ph\]](#).
- [22] C. Lorcé, A. Metz, B. Pasquini, and S. Rodini, “Energy-momentum tensor in QCD: nucleon mass decomposition and mechanical equilibrium,” *JHEP* **11** (2021) 121, [arXiv:2109.11785 \[hep-ph\]](#).
- [23] B. Duran *et al.*, “Determining the gluonic gravitational form factors of the proton,” *Nature* **615** no. 7954, (2023) 813–816, [arXiv:2207.05212 \[nucl-ex\]](#).
- [24] R. Abdul Khalek *et al.*, “Science Requirements and Detector Concepts for the Electron-Ion Collider: EIC Yellow Report,” *Nucl. Phys. A* **1026** (2022) 122447, [arXiv:2103.05419 \[physics.ins-det\]](#).
- [25] A. Accardi *et al.*, “Strong Interaction Physics at the Luminosity Frontier with 22 GeV Electrons at Jefferson Lab,” [arXiv:2306.09360 \[nucl-ex\]](#).
- [26] V. Bertone, H. Dutrieux, C. Mezrag, H. Moutarde, and P. Sznajder, “Deconvolution problem of deeply virtual Compton scattering,” *Phys. Rev. D* **103** no. 11, (2021) 114019, [arXiv:2104.03836 \[hep-ph\]](#).
- [27] E. Moffat, A. Freese, I. Cloët, T. Donohoe, L. Gamberg, W. Melnitchouk, A. Metz, A. Prokudin, and N. Sato, “Shedding light on shadow generalized parton distributions,” *Phys. Rev. D* **108** no. 3, (2023) 036027, [arXiv:2303.12006 \[hep-ph\]](#).
- [28] D. Mueller and A. Schafer, “Complex conformal spin partial wave expansion of generalized parton distributions and distribution amplitudes,” *Nucl. Phys. B* **739** (2006) 1–59, [arXiv:hep-ph/0509204](#).
- [29] V. M. Braun, A. N. Manashov, S. Moch, and M. Strohmaier, “Three-loop evolution equation for flavor-nonsinglet operators in off-forward kinematics,” *JHEP* **06** (2017) 037, [arXiv:1703.09532 \[hep-ph\]](#).



- [30] V. M. Braun, A. N. Manashov, and B. Pirnay, “Finite- $t$  and target mass corrections to DVCS on a scalar target,” *Phys. Rev. D* **86** (2012) 014003, [arXiv:1205.3332 \[hep-ph\]](#).
- [31] V. M. Braun, A. N. Manashov, and B. Pirnay, “Finite- $t$  and target mass corrections to deeply virtual Compton scattering,” *Phys. Rev. Lett.* **109** (2012) 242001, [arXiv:1209.2559 \[hep-ph\]](#).
- [32] V. M. Braun, A. N. Manashov, D. Müller, and B. M. Pirnay, “Deeply Virtual Compton Scattering to the twist-four accuracy: Impact of finite- $t$  and target mass corrections,” *Phys. Rev. D* **89** no. 7, (2014) 074022, [arXiv:1401.7621 \[hep-ph\]](#).
- [33] V. M. Braun, A. N. Manashov, S. Moch, and M. Strohmaier, “Two-loop evolution equations for flavor-singlet light-ray operators,” *JHEP* **02** (2019) 191, [arXiv:1901.06172 \[hep-ph\]](#).
- [34] V. M. Braun, A. N. Manashov, S. Moch, and M. Strohmaier, “Three-loop off-forward evolution kernel for axial-vector operators in Larin’s scheme,” *Phys. Rev. D* **103** no. 9, (2021) 094018, [arXiv:2101.01471 \[hep-ph\]](#).
- [35] V. M. Braun, K. G. Chetyrkin, and A. N. Manashov, “NNLO anomalous dimension matrix for twist-two flavor-singlet operators,” *Phys. Lett. B* **834** (2022) 137409, [arXiv:2205.08228 \[hep-ph\]](#).
- [36] V. M. Braun, Y. Ji, and A. N. Manashov, “Next-to-leading-power kinematic corrections to DVCS: a scalar target,” *JHEP* **01** (2023) 078, [arXiv:2211.04902 \[hep-ph\]](#).
- [37] S. Moch and S. Van Thurenhout, “Renormalization of non-singlet quark operator matrix elements for off-forward hard scattering,” *Nucl. Phys. B* **971** (2021) 115536, [arXiv:2107.02470 \[hep-ph\]](#).
- [38] S. Van Thurenhout, “Off-forward anomalous dimensions of non-singlet transversity operators,” *Nucl. Phys. B* **980** (2022) 115835, [arXiv:2204.02140 \[hep-ph\]](#).
- [39] A. V. Vinnikov, “Code for prompt numerical computation of the leading order GPD evolution,” [arXiv:hep-ph/0604248](#).
- [40] B. Berthou *et al.*, “PARTONS: PARTonic Tomography Of Nucleon Software: A computing framework for the phenomenology of Generalized Parton Distributions,” *Eur. Phys. J. C* **78** no. 6, (2018) 478, [arXiv:1512.06174 \[hep-ph\]](#).
- [41] A. Freund and M. F. McDermott, “Next-to-leading order evolution of generalized parton distributions for DESY HERA and HERMES,” *Phys. Rev. D* **65** (2002) 056012, [arXiv:hep-ph/0106115](#). [Erratum: *Phys.Rev.D* 66, 079903 (2002)].
- [42] K. Kumericki, D. Mueller, and K. Passek-Kumericki, “Towards a fitting procedure for deeply virtual Compton scattering at next-to-leading order and beyond,” *Nucl. Phys. B* **794** (2008) 244–323, [arXiv:hep-ph/0703179](#).
- [43] K. Kumerički, “Gepard: Tool for studying the 3d quark and gluon distributions in the nucleon,”. <https://gepard.phy.hr/credits.html>.  
<https://gepard.phy.hr/credits.html>.
- [44] V. Bertone, H. Dutrieux, C. Mezrag, J. M. Morgado, and H. Moutarde, “Revisiting evolution equations for generalised parton distributions,” *Eur. Phys. J. C* **82** no. 10, (2022) 888, [arXiv:2206.01412 \[hep-ph\]](#).
- [45] A. V. Belitsky, A. Freund, and D. Mueller, “NLO evolution kernels for skewed transversity distributions,” *Phys. Lett. B* **493** (2000) 341–349, [arXiv:hep-ph/0008005](#).

- [46] V. Bertone, S. Carrazza, and J. Rojo, “APFEL: A PDF Evolution Library with QED corrections,” *Comput. Phys. Commun.* **185** (2014) 1647–1668, [arXiv:1310.1394 \[hep-ph\]](#).
- [47] V. Bertone, “APFEL++: A new PDF evolution library in C++,” *PoS DIS2017* (2018) 201, [arXiv:1708.00911 \[hep-ph\]](#).
- [48] V. M. Braun, A. N. Manashov, and B. Pirnay, “Scale dependence of twist-three contributions to single spin asymmetries,” *Phys. Rev. D* **80** (2009) 114002, [arXiv:0909.3410 \[hep-ph\]](#). [Erratum: *Phys.Rev.D* 86, 119902 (2012)].
- [49] P. Kroll and K. Passek-Kumerički, “Transition GPDs and exclusive electroproduction of  $\pi$ - $\Delta$ (1232) final states,” *Phys. Rev. D* **107** no. 5, (2023) 054009, [arXiv:2211.09474 \[hep-ph\]](#).
- [50] A. V. Belitsky, X. Ji, and F. Yuan, “Final state interactions and gauge invariant parton distributions,” *Nucl. Phys. B* **656** (2003) 165–198, [arXiv:hep-ph/0208038](#).
- [51] G. Altarelli and G. Parisi, “Asymptotic Freedom in Parton Language,” *Nucl. Phys. B* **126** (1977) 298–318.
- [52] F. Delduc, M. Gourdin, and E. G. Oudrhiri-Safiani, “Photon Structure Functions in Quantum Chromodynamics. 2. Feynman Diagram Method,” *Nucl. Phys. B* **174** (1980) 157–165.
- [53] X. Artru and M. Mekhfi, “Transversely Polarized Parton Densities, their Evolution and their Measurement,” *Z. Phys. C* **45** (1990) 669.
- [54] W. Vogelsang, “Q\*\*2 evolution of spin dependent parton densities,” *Acta Phys. Polon. B* **29** (1998) 1189–1200, [arXiv:hep-ph/9805295](#).
- [55] G. P. Lepage and S. J. Brodsky, “Exclusive Processes in Perturbative Quantum Chromodynamics,” *Phys. Rev. D* **22** (1980) 2157.
- [56] E. Leader and C. Lorcé, “The angular momentum controversy: What’s it all about and does it matter?,” *Phys. Rept.* **541** no. 3, (2014) 163–248, [arXiv:1309.4235 \[hep-ph\]](#).
- [57] C. Lorcé, L. Mantovani, and B. Pasquini, “Spatial distribution of angular momentum inside the nucleon,” *Phys. Lett. B* **776** (2018) 38–47, [arXiv:1704.08557 \[hep-ph\]](#).
- [58] S. V. Goloskokov and P. Kroll, “Vector meson electroproduction at small Bjorken-x and generalized parton distributions,” *Eur. Phys. J. C* **42** (2005) 281–301, [arXiv:hep-ph/0501242](#).
- [59] S. V. Goloskokov and P. Kroll, “The Role of the quark and gluon GPDs in hard vector-meson electroproduction,” *Eur. Phys. J. C* **53** (2008) 367–384, [arXiv:0708.3569 \[hep-ph\]](#).
- [60] S. V. Goloskokov and P. Kroll, “An Attempt to understand exclusive  $\pi^+$  electroproduction,” *Eur. Phys. J. C* **65** (2010) 137–151, [arXiv:0906.0460 \[hep-ph\]](#).
- [61] G. Curci, W. Furmanski, and R. Petronzio, “Evolution of Parton Densities Beyond Leading Order: The Nonsinglet Case,” *Nucl. Phys. B* **175** (1980) 27–92.